Molecular and Cellular Endocrinology 350 (2012) 99–106

Contents lists available at SciVerse ScienceDirect

Molecular and Cellular Endocrinology

journal homepage: www.elsevier.com/locate/mce

Synergistic anti-tumor effects of RAD001 with MEK inhibitors in neuroendocrine tumors: A potential mechanism of therapeutic limitation of mTOR inhibitor

Shinya Iida, Yasuhiro Miki, Katsuhiko Ono, Jun-ichi Akahira, Yasuhiro Nakamura, Takashi Suzuki, Hironobu Sasano *

Department of Pathology, Tohoku University Graduate School of Medicine, Sendai, Japan

ARTICLE INFO

Article history:
Received 15 June 2011
Received in revised form 25 October 2011
Accepted 25 November 2011
Available online 8 December 2011

Keywords:
Neuroendocrine tumors
Mammalian target of rapamycin
Mitogen-activated protein kinase
Signal transduction

ABSTRACT

Mammalian target of rapamycin (mTOR) inhibitors have been clinically used as anticancer agents in several types of human malignancies including neuroendocrine tumor (NET) but the development of clinical resistances or their therapeutic limitations have been also reported. This clinical resistance has been proposed to be partly due to a compensatory activation of an mTOR upstream factor Akt and MEK/ERK pathway in NET cells but its details have not necessarily been reported. Therefore, in this study, we examined the effects of mTOR inhibitors on these activations and of the concomitant treatment of mTOR and MEK inhibitors in two NET cell lines, NCI-H727 and COLO320. We evaluated the effects of RAD001, mTOR inhibitor, and U0126, MEK inhibitor, on cell proliferation and migration of these cells. In addition, an alteration of the factors involved in Akt/mTOR and MEK/ERK pathways was also examined under administration of these agents. RAD001 and U0126 treatment significantly inhibited cell proliferation and their combined treatment synergistically decreased it in both cell lines. Additionally, these treatments above decreased the expression of cell cycle-related factors, suggestive of an involvement of cell cycle arrest in therapeutic effects. The combined treatment also inhibited the cell migration in NCI-H727 via the decrement of MMP2 and 9 in an additive manner. We demonstrated the potential synergistic/combined effects of inhibitors of mTOR and MEK on cell proliferation and migration. These results suggest the potential therapeutic efficacy of the combined therapy of mTOR and MEK inhibitors or a dual inhibitor for the treatment of NET patients.

1. Introduction

Mammalian target of rapamycin (mTOR) plays a pivotal role in the regulation of several cell functions such as cell proliferation, survival, translation and metabolism (Bjornsti and Houghton, 2004; Pouysségur et al., 2006; Wullschleger et al., 2006). mTOR is a central regulator in phosphatidylinositol 3-kinase (PI3K)/Akt/mTOR pathway under receptor tyrosine kinases (RTKs) and has been recently examined as a novel therapeutic target for human neoplasms including neuroendocrine tumor (NET) because this pathway is commonly over-activated in NET (Ciuffreda et al., 2010). In addition, we and other investigators also reported the association between the overactivation of this pathway and insulin-like growth factor-1 receptor (IGF-1R) or epidermal growth factor receptor (EGFR) in NET (Iida et al., 2010; von Wichert et al., 2000; Zutzmann et al., 2007).

mTOR is composed of two complexes, mTOR complex 1 (mTORC1) and mTORC2, in terms of the functional activity (Thomson et al., 2009). mTORC1 inhibitors, rapamycin and its analogues (rapalogs), have been considered to demonstrate immunosuppressive and antitumor activities through the following mechanisms: rapalogs first bind to immunophilin FK506-binding protein 12 (FKBP12) and this complex subsequently binds to mTORC1, not to mTORC2, which results in an inhibition of downstream signaling pathways (Jayaraman and Marks, 1993; Loewith et al., 2002; Vilella-Bach et al., 1999). The detailed function of mTORC2 has not been well-characterized mainly because mTORC2 is insensitive to rapalogs and mTORC2-specific inhibitors are not still available at this juncture. Rapalogs, including CCI-779 (Wyeth), AP23573 (ARIAD Pharmaceuticals Inc.), and RAD001 (everolimus; Novartis AG), have been used in various clinical trials as an antitumor agent alone against various tumor types. For example, rapalogs demonstrated marked clinical therapeutic effects and relatively satisfactory safety profiles as a single agent in advanced renal cell carcinoma (Phase III) and mantle-cell lymphoma (Phase III) (Amato et al., 2009; Hess et al., 2009; Vilella-Bach et al., 1999). As for the patients with metastatic pancreatic

* Corresponding author. Address: Department of Pathology, Tohoku University Graduate School of Medicine, 2-1 Seiryo-machi, Aoba-ku, Sendai, Miyagi 980-8575, Japan. Tel.: +81 22 717 8050; fax: +81 22 717 8051.
E-mail address: hsasano@patholo2.med.tohoku.ac.jp (H. Sasano).

0303-7207/$ - see front matter © 2011 Elsevier Ireland Ltd. All rights reserved.
doi:10.1016/j.mce.2011.11.024

NET, Phase III clinical trials are also being carried out (Chan et al., 2010; Yao et al., 2011). It is, however, also true that results of these clinical trials employing this as a single agent or in combination with chemotherapeutic agents turned to be less successful than expected, which could limit its antitumor activity in clinical settings.

Recently, two potential mechanisms of the limitations or resistances to mTOR inhibition have been proposed. O'Reilly et al. (2006) reported that mTOR inhibition resulted in an activation of Akt, an upstream factor of mTOR, through upregulation of RTKs or of its substrates such as PDGFRs and IRS-1 (Hartley and Cooper, 2002; Zhang et al., 2007). Octreotide, which has been widely used for the treatment of NET patients, has been reported to decrease Akt phosphorylation (Charland et al., 2001; Theodoropoulou et al., 2006) and the effects of combination with rapalogs and octreotide were also evaluated against NET in both preclinical and clinical settings (Grozinsky-Glasberg et al., 2008; Moreno et al., 2008; Yao et al., 2008; Pavel et al., 2011). Results of these studies above all indicated that mTOR inhibitors were associated with significant antiproliferative activities but octreotide itself was not necessarily associated with sufficient antiproliferative effects as a single agent. Therefore, the clinical significance of additive effects of the combined treatment of mTOR inhibitors and octreotide has still remained in dispute.

The great majority of the studies exploring the limitation or resistance of antitumor effects of rapalogs studied their correlation with PI3K/Akt signaling pathway but several investigators reported that mTOR inhibition resulted in an activation of the MEK/ERK cascade through a PI3K-dependent feedback loop (Carracedo et al., 2008; Mi et al., 2009; Wang et al., 2008). In these studies, the combined treatment of both mTOR and MEK inhibitors improved the growth inhibitory effects of mTOR inhibition both *in vitro* and *in vivo* in various types of human malignancies. The dual inhibition of Ras/Raf/MEK/ERK and PI3K/Akt/mTOR pathways has also been reported as a potential anti-neoplastic therapy in glioma (Hjelmeland et al., 2007), prostate cancer (Kikade et al., 2008), melanoma (Lasithiotakis et al., 2008), thyroid cancer (Jin et al., 2009), pancreatic cancer (Chang et al., 2010) and glioblastoma (Sunayama et al., 2010). However, it is also true that the association between PI3K/Akt/mTOR and MEK/ERK pathways in NET cells has not been studied in details. Therefore, in this study, we hypothesized that the combined or synergistic effects of a dual inhibition of mTOR and MEK may result in a better therapeutic outcome in NET patients and evaluated this possibility using NET cell lines.

2. Materials and methods

2.1. Cell culture and reagents

NCI-H727, a human bronchial NET cell line, was purchased from the American Type Culture Collection (Manassas, VA, USA). COLO320-DM (COLO320) has been generally used as a human colon adenocarcinoma having neuroendocrine characteristics (Quinn et al., 1979) and we used this cell line in this study. This was purchased from The Health Science Research Resources Bank (Osaka, Japan). These cells were cultured in RPMI-1640 medium (Sigma Aldrich Co., St. Louis, MO, USA) containing 10% fetal bovine serum (FBS; Nichirei Co., Ltd., Tokyo, Japan). MEK inhibitor U0126 ethanolate (1,4-diamino-2,3-dicyano-1,4-bis[2-aminophenylthio]-butadiene) was purchased from Sigma Aldrich and RAD001 (everolimus) was kindly provided from Novartis AG (Basel, Switzerland). These reagents were dissolved in DMSO.

2.2. Antibodies

Primary antibodies employed in immunocytochemistry were as follows: anti-chromogranin A, anti-neuron specific enolase (NSE) and anti-synaptophysin (Dako, Glostrup, Denmark). For immunoblot analysis, the following antibodies were used (all from Cell Signaling Technology except where indicated): anti-Akt (#4685) and anti-phospho-Ser473-Akt (#4060), anti-mTOR (#2983) and anti-phospho-Ser2448-mTOR (#2971), anti-RpS6 (S6; #2217) and anti-phospho-Ser240/244 RpS6 (#2215), anti-4EBP1 (#9644) and anti-phospho-Thr70-4EBP1 (#9455), anti-p44/42 MAPK (ERK; #4695) and anti-phospho-Thr202/Tyr204-p44/42 MAPK (#4376), anti-Cyclin D1 (Dako Cytomation, Glostrup, Denmark), anti-Cyclin B1 (SantaCruz Biotechnology, Santa Cruz, CA) and anti-β-actin (Sigma Aldrich).

2.3. Immunocytochemistry

The cells were cultured in the 4-well slide (Nalge Nunc International) until reaching 80–90% confluence and then the slides were fixed with 10% formalin for 5 min at room temperature. Immunocytochemistry was performed as we previously reported (Iida et al., 2010). The cells were immunostained by a biotin–streptavidin method using Histofine kit (Nichirei Co., Ltd., Tokyo, Japan; chromogranin A and synaptophysin) and EnVision$^+$ method (Dako; NSE). The antigen–antibody complex was subsequently visualized with 3,3'-diaminobenzidine (DAB) solution (Dako Liquid DAB + Substrate System; Dako) and counterstained with hematoxylin.

2.4. Cell proliferation assay

The status of cell proliferation of NCI-H727 and COLO320 cells was determined using WST-8 [2-(2-methoxy-4-nitrophenyl)-3-(4-nitrophenyl)-5-(2,4-disulfophenyl)-2H-tetrazolium monosodium salt] method (Cell Counting Kit-8; Dojindo Inc., Kumamoto, Japan). The methods were based upon those which we previously reported (Iida et al., 2010).

2.5. Evaluation of combination index

In order to determine whether the combined effects were additive, synergistic or antagonistic, proliferation assay was conducted as follows: both RAD001 and U0126 were simultaneously administered at the ratio of 1:10 (NCI-H727) or 1:100 (COLO320) for 3 days. We analyzed the combination effects or "synergism" based upon the combination index (CI) method of Chou and Talalay (Chou and Talalay, 1984; Chou, 2006, 2010) using CalcuSyn software (version 2.0; Biosoft, Cambridge, UK). $CI < 1.0$ indicates synergism, $CI = 1.0$ indicates additivity and $CI > 1.0$ indicates antagonism.

2.6. Immunoblot analysis

Both NCI-H727 and COLO320 were treated with each single reagent or their combination conditions for adequate length of time and the total protein of the cells was extracted using PhosphoSafe™ Extraction Reagent (Biosciences Inc., Darmstadt, Germany). Following the measurement of protein concentration (Protein Assay Kit Wako: Wako), the total protein was individually subjected to SDS–PAGE (SuperSep™Ace: Wako). The proteins were then transferred onto Hybond P polyvinylidene difluoride membrane (GE Healthcare, Buckinghamshire, UK). The membranes were then blocked in 5% non-fat dry skim milk powder (Wako) for over 1 h at room temperature, and were then incubated with primary antibodies for 24–48 h at 4 °C using ImmunoShot (Cosmo Bio Co., Ltd., Tokyo, Japan). The working dilutions of the primary antibodies used in this study were summarized as follows: mTOR, Akt, S6, 4EBP1, ERK and β-actin, 1/1000; phosphorylated mTOR (p-mTOR), p-Akt, p-S6, p-4EBP1, p-ERK and Cyclin B1, 1/500; Cyclin D1, 1/250.

These antibody–protein complexes on the blots were detected using ECL-plus Western blotting detection reagents (GE Healthcare) following incubation with anti-mouse or anti-rabbit IgG horseradish peroxidase (GE Healthcare) at room temperature. The corresponding protein bands were subsequently visualized and analyzed using LAS-1000 cooled CCD-camera chemiluminescent image analyzer and Multi Gauge v3.1 software (both from Fuji Photo Film Co., Ltd., Tokyo, Japan), respectively.

2.7. Wound healing assay

We employed wound healing assay (Liang et al., 2007) in order to evaluate the *in vitro* migration of NCI-H727 cells. The confluent cell layer was scratched with a sterile plastic P-200 pipette tip. The cells migrated into these scratched areas were evaluated under light microscopy. The areas of these foci of wound closure in each culture conditions were quantified using MultiGauge v3.1 software (Fuji Photo Film Co., Ltd.) and compared to the corresponding areas in control cells.

2.8. Quantitative reverse transcriptional-polymerase chain reaction (RT-PCR)

Total RNA was extracted from NCI-H727 treated with RAD001 and/or U0126 for 12 h using TRIZOL reagent (Invitrogen, CA, USA) and a reverse transcriptional reaction was conducted using a QuantiTect reverse transcription kit (Qiagen, Hilden, Germany) and a PTC-200 Peltier Thermal Cycler DNA Engine (MJ Research Inc., Watertown, MA). Real-time PCR was carried out using the LightCycler System (Roche Diagnostics, Mannheim, Germany) and a QuantiTect SYBR Green PCR Master Mix (Qiagen). The primer sequences were summarized in Table 1. The ribosomal protein L13A (RPL13A) was used as an internal control and mRNA level of each condition was calculated as a ratio of *RPL13A* level compared with control levels.

2.9. Statistical analysis

The statistical analysis about the results of proliferation assay and wound healing assay was analyzed with Scheffe test (StatView 5.0J software, SAS Institute Inc., NC, USA) and Student *t* test (Microsoft Excel). Statistical significance was defined as $P < 0.05$.

3. Results

3.1. Expression of neuroendocrine markers in NET cell lines

We first confirmed the neuroendocrine features of two NET cell lines NCI-H727 and COLO320 used in our present study using immunocytochemistry. We examined three neuroendocrine markers chromogranin A, NSE and synaptophysin and all of these markers were detected in the cytoplasm of both cell lines (Fig. 1).

Table 1
Sequences of primers in this study.

Gene	GenBank No.	PCR primers
MMP2	NM_001127891	5′-ATAACCTGGATGCCGTCGTG-3′ 5′-AGCCTAGCCAGTCGGATTTG-3′
MMP9	NM_004994	5′-GACGTCTTCCAGTACCGA-3′ 5′-GGATGTCATAGGTCACGTAGC-3′
RPL13A	NM_012423	5′-CCTGGAGGAGAAGAGGAAAG-3′ 5′-TTGAGGACCTCTGTGTATTT-3′

3.2. Antitumor efficacy of RAD001 and MEK inhibitors in NET cell lines

We examined the anti-tumor effects and their concentration-dependency of RAD001 and U0126 in NCI-H727 and COLO320 (Fig. 2A and B, respectively). RAD001 significantly decreased the number of cells at 9th day of treatment in NCI-H727 and at 3rd day in COLO320 in the range of 1–100 nM, compared to the control levels (Fig. 2A). As for U0126, the cell growth was significantly inhibited at 3rd day with 1 μM in NCI-H727 and with 100 nM and 10 μM in COLO320 (Fig. 2B). Therefore, based upon these results, we determined the concentrations of these reagents as follows: RAD001, 100 nM; U0126, 1 μM (NCI-H727) or 10 μM (COLO320). The combined treatment of RAD001 with U0126 demonstrated a significant inhibition in both NCI-H727 and COLO320 for 3 days, compared to the other groups (Fig. 2C). Additionally, CI values in all conditions were smaller than 1.0 in both of the cell lines studied (Table 2).

3.3. Intracellular mechanisms of synergistic effects of mTOR and MEK inhibitors in NET cell lines

We demonstrated the synergic inhibition of cell proliferation by combined treatment of mTOR inhibitors with MEK inhibitors as described above. We then examined the status of the factors involved in Akt/mTOR and MEK/ERK signaling pathways at protein levels in order to clarify the alterations of signal transduction factors expression following the treatment. We first examined the time-dependency and determined the adequate time of simultaneous treatment in two of NET cell lines (NCI-H727, 6 h; COLO320, 3 h; data not shown). The status of mTOR-related factor expression was subsequently evaluated and the results were summarized as follows (Fig. 3): (a) RAD001 markedly inhibited the phosphorylation of mTOR and its downstream factors, S6 and 4EBP1, and U0126 also inhibited that of ERK. (b) RAD001 induced an activation of Akt and ERK. (c) U0126 similarly induced the expression of p-Akt and p-mTOR, especially in COLO320, but decreased that of p-S6 and p-4EBP1. (d) The combined treatment inhibited both RAD001-induced ERK activation and U0126-induced mTOR activation and demonstrated additive inhibition of the phosphorylation of both S6 and 4EBP1.

3.4. Effects of the treatment on cell cycle related protein expression

In order to investigate the effects of the combined treatment on cell cycle, we detected cell cycle related proteins when simultaneously treated. In NCI-H727 cells, RAD001 treatment induced the expression of Cyclin D1, which was inhibited or decreased by U0126 treatment such as phospho-ERK expression (Fig. 4). However, both reagents suppressed the expression of Cyclin D1 in COLO320. Regarding Cyclin B1, both RAD001 and U0126 treatment decreased its expression and their combination resulted in further reduction.

3.5. Effects of the treatment on cell migration activity

Results of wound healing assay demonstrated that cell migration activities were suppressed in single reagent treated cells (Fig. 5A) and the combined treatment resulted in significantly higher inhibition/suppression of cell migration than single treatment ($P < 0.05$: Fig. 5B).

3.6. Effects of the treatment on MMPs mRNA expression

We examined the effects of these reagents on MMP2 and MMP9 expressions at mRNA levels in NCI-H727 in order to investigate the mechanisms of the inhibition of cell migration as demonstrated

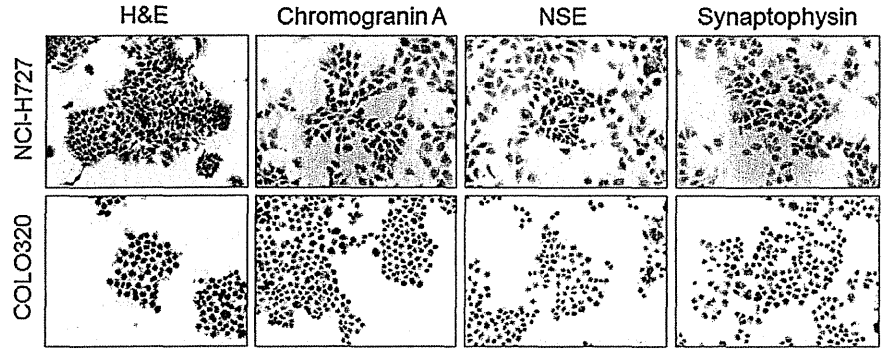

Fig. 1. Representative illustration of hematoxylin and eosin (H&E) staining and immunocytochemistry of neuroendocrine markers in NET cell lines. Both NCI-H727 and COLO320 cultured in 4-well plate were immunostained with three neuroendocrine markers, chromogranin A, NSE and synaptophysin. Original magnification, 100×.

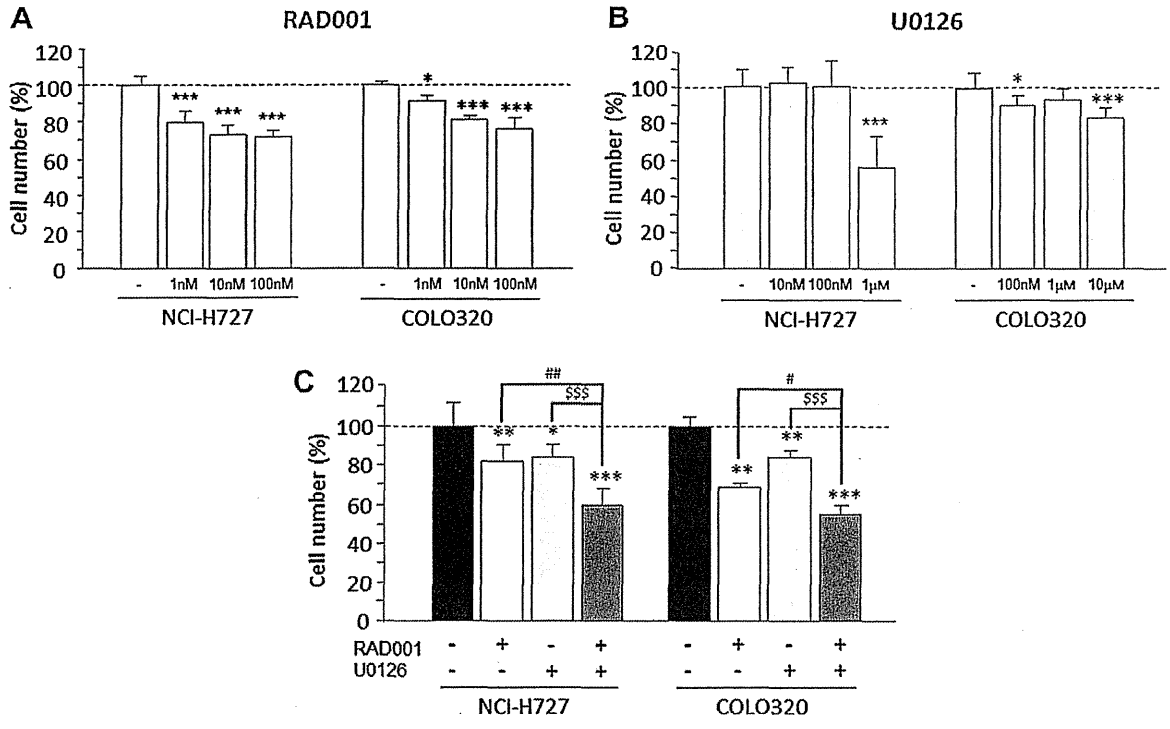

Fig. 2. Anti-tumor effects of RAD001 and U0126 treatment in NET cells. (A) RAD001 treatment (1–100 nM) in NCI-H727 at 9th day and in COLO320 at 3rd day. (B) U0126 treatment at the range of 10 nM to 1 μM in NCI-H727 and 100 nM to 10 μM in COLO320. (C) Combination treatment of RAD001 (100 nM) with U0126 [1 μM (NCI-H727) or 10 μM (COLO320)] at 3rd day. All data are shown as mean ($n = 6$). Error bars indicate SD. Statistical significances were calculated by Scheffe test. $^{*}P < 0.05$, $^{**}P < 0.01$ and $^{***}P < 0.001$, compared with control group; $^{\#}P < 0.05$ and $^{\#\#}P < 0.01$, compared with RAD001 treatment group; $^{\$\$\$}P < 0.001$, compared with U0126 treatment group.

above. Results were summarized in Fig. 6. RAD001 exerted no significant effects upon *MMP2* mRNA expression, whereas U0126 and the combination treatment significantly decreased that of MMP2. As for MMP9, both RAD001 and U0126 significantly decreased its expression and their simultaneous administration decreased it in an additive manner.

4. Discussion

We previously reported the subclassification of non-functioning NET cases using hierarchical clustering analysis based upon immunoreactivity of various factors involved in the regulation of cell proliferation (Iida et al., 2010). Briefly, non-functioning NETs were sub-classified into sstr-related group and mTOR activation-related group and the latter group may be considered to benefit from mTOR inhibitors. It is, however, also true that several investigators reported the potential limitation of the efficacy of mTOR inhibitors in NET cases (Duran et al., 2006). In our present study, we focused

Table 2
Combination index values of the combined effects of RAD001 with U0126 in NET cells.

Cell line	RAD001	U0126	Fractional affected	CI value
NCI-H727	1 nM	10 nM	0.266	0.003
	10 nM	100 nM	0.301	0.021
	100 nM	1 μM	0.402	0.144
COLO320	1 nM	100 nM	0.205	0.098
	10 nM	1 μM	0.289	0.089
	100 nM	10 μM	0.453	0.453

Note: CI < 1.0 indicates synergism, CI = 1.0 indicates additivity and CI > 1.0 indicates antagonism.

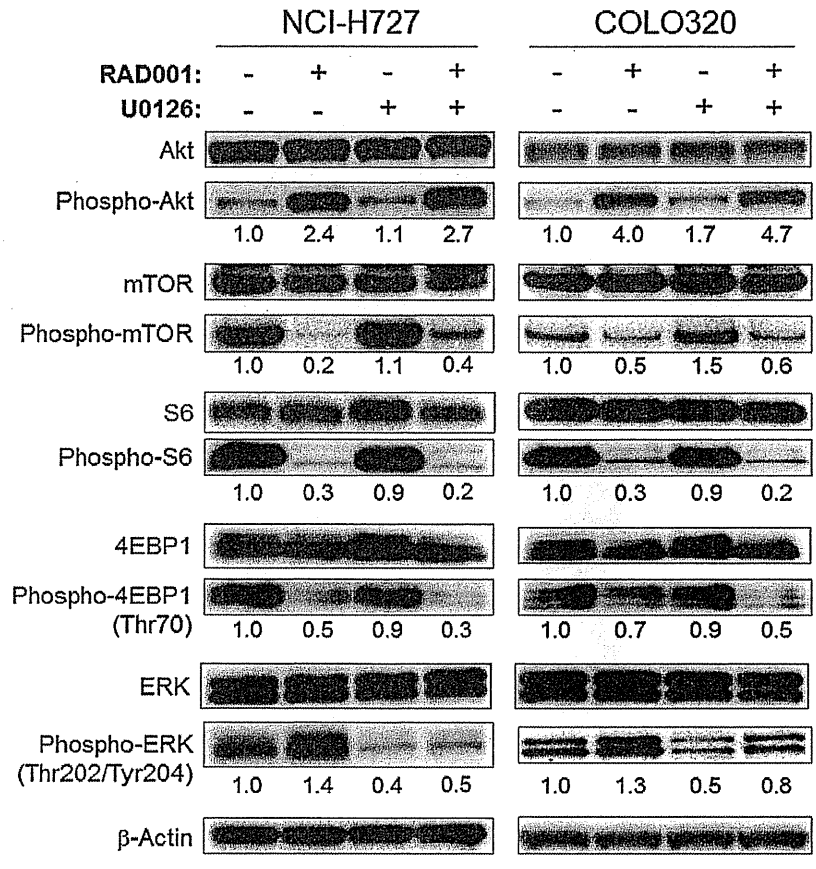

Fig. 3. Summary of the expression of phosphorylated factors in Akt/mTOR and MEK/ERK pathway when RAD001 and/or U0126 were treated. Phosphorylated forms of Akt, mTOR, S6, 4EBP1 and ERK were detected when RAD001 (100 nM) and U0126 [1 μM (NCI-H727) or 10 μM (COLO320)] were treated in NCI-H727 for 6 h and COLO320 for 3 h. The number under each band calculated using MultiGauge v3.1 software (Fuji Photo Film Co., Ltd.) indicated the intensity when the control bands were 1.0.

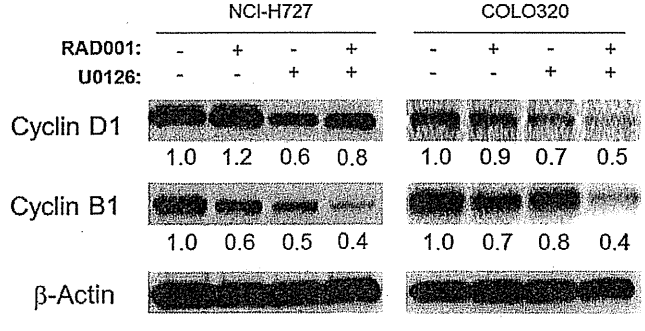

Fig. 4. Summary of the expression of cell cycle-related factors when RAD001 and/or U0126 were administered. The expressions of Cyclin D1 and Cyclin B1 as G1/S and G2/M phase markers, respectively, were detected when treated with RAD001 (100 nM) and U0126 [1 μM (NCI-H727) or 10 μM (COLO320)] for 24 h. The number under each band calculated using MultiGauge v3.1 software (Fuji Photo Film Co., Ltd.) indicated the intensity when the control bands were 1.0.

on one of the potential mechanisms of development of resistance to mTOR inhibitors, that is, a positive feedback loop from MEK/ERK pathway (Carracedo et al., 2008; Mi et al., 2009; O'Reilly et al., 2006; Wang et al., 2008) because the combined therapeutic effects of mTOR and MEK inhibitors has not been necessarily studied in NET.

The mechanism of therapeutic resistance to an inhibitor of Raf, an upstream factor of MEK, was recently reported in melanoma cells (Johannessen et al., 2010; Nazarian et al., 2010). These reports also indicated an involvement of the acquired resistance through activating a RTK (PDGFRβ was found in this study)-dependent survival pathway and reactivating MAPK pathway via Ras upregulation. In addition, U0126 has been known to cause an activation of PI3K/Akt/mTOR pathway in non-small cell lung carcinoma cells, as was previously reported by Meng et al. (2009). They also demonstrated the association of high levels of Akt activity with resistances to MEK inhibition. In our present study, single treatment of mTOR or MEK inhibitor resulted in a significant suppression of cell proliferation and their combination did demonstrate therapeutic effects in a synergistic manner because its CI values were smaller than 1.0. We first demonstrated that RAD001 inhibited an activation of mTOR but did activate Akt and ERK at the protein levels in both cell lines. As for MEK inhibition, U0126 suppressed ERK activation but did activate Akt and mTOR. These results indicated that between these two pathways, one induced the other pathway and the combined treatment inhibited the each pathway induced by the each reagent as expected. In addition, U0126 inhibited the activation of both S6 and 4EBP1, downstream factors of mTOR, as RAD001 did. Both of these factors have been known to be regulated by MEK/ERK pathway, as previously reported (Herbert et al., 2002; Wang et al., 2001). Zitzmann et al. previously demonstrated the combination treatment of RAD001 with a Raf inhibitor Raf265 in NET cells (Zitzmann et al., 2010). In our present study, RAD001 increased the activation of Akt but not that of ERK at the concentration of 100 nM for 2 and 24 h in NCI-H727, respectively. We examined the antitumor effects of RAD001 in a time-dependent manner and detected ERK activation by the treatment of this reagent for 3, 6 and 12 h (data not shown). In addition, ERK activation

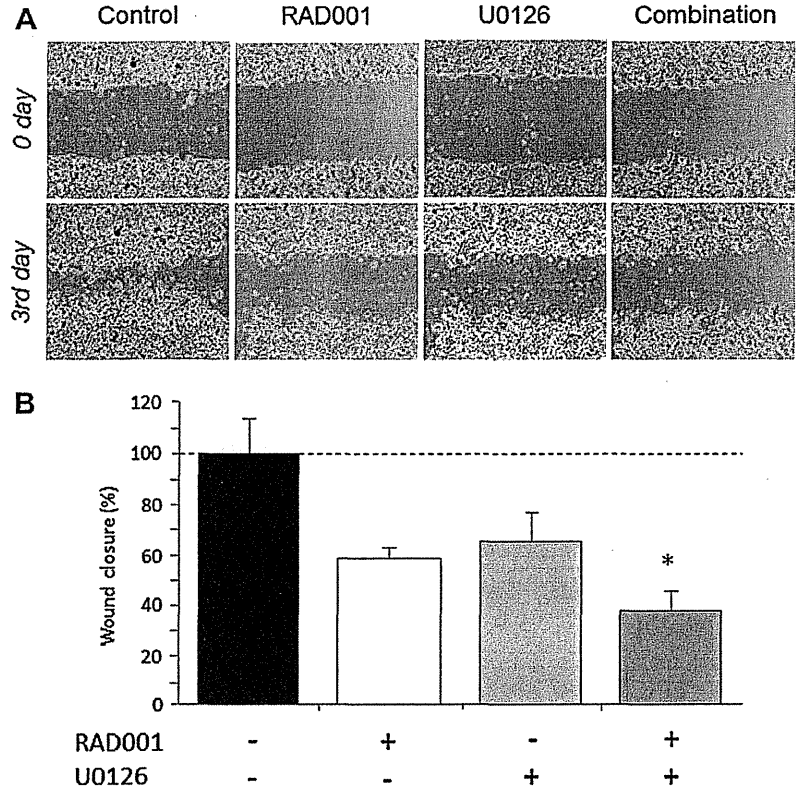

Fig. 5. Summary of the results of migration assay in NCI-H727. (*A*) Representative illustrations of migration assay in NCI-H727 at the 3rd day and (*B*) the results of statistical analysis ($P < 0.05$, Scheffe test; $n = 3$).

was detected when RAD001 and mTOR/PI3K inhibitor NVP-BEZ235 were treated in other types of NET cell lines (i.e. BON1 and GOT1). Zitzmann et al. also demonstrated that Raf265 induced Akt activation, suggesting that, as described in our present study, an inhibition of Ras–Raf–MEK–ERK pathway may result in a positive feedback loop for PI3K–Akt–mTOR pathway. These results all indicated that the combined inhibition of both pathways could be effective in NET cells.

It is widely known that both mTOR and MEK inhibitors induce cell cycle arrest (Hoshino et al., 2001; Yu et al., 2001). Therefore, in this study, we explored alterations of the factors involved in the process of cell cycle arrest. Cell cycle was arrested by an administration of a single inhibitor and furthermore, the combined treatment additively suppressed the expression of G1/S and G2/M phase positive regulators, Cyclin D1 and Cyclin B1, respectively. These results all indicated that the anti-tumor activity of this dual inhibition of mTOR and MEK pathway was caused by the cell cycle arrest. We further demonstrated the differences of their effects on Cyclin D1 expression between in two types of NET cells. In NCI-H727 cell line, U0126 decreased the expression of Cyclin D1, whereas RAD001 induced its amount to the similar level of phospho-ERK. These findings suggested that Cyclin D1 expression was predominantly regulated by MEK/ERK pathway in NCI-H727, as previously reported by Lavoie et al. (1996).

Some patients with well-differentiated non-functioning NETs may clinically present with metastatic disease at initial visits and therapeutic options in these cases are markedly limited (Reidy et al., 2009). No standard therapy is currently available, which makes it important to explore the possibility of the combined treatment studied in our present *in vitro* study of NET cells. In glioma cells, the combination of a Raf inhibitor and RAD001 significantly suppressed the invasive properties of tumor cells (Hjelmeland et al., 2007). In our present study, the combination of RAD001 and U0126 significantly decreased NET cell migration in addition to synergistic inhibition of cell proliferation, which may also suggest an additional benefit of the combination of mTOR and MEK inhibitors for the treatment of NET patients. In our present study, we focused on MMPs expression involved in the inhibitory mechanisms of cell migration. In Lewis lung carcinoma cells, *MMP2* mRNA expression was not influenced by mTOR inhibitor rapamycin and MEK inhibitor decreased its expression as we demonstrated in NCI-H727 (Zhang et al., 2004). As for MMP9, its expression was reported to be significantly correlated with PI3K–Akt–mTOR pathway in hepatocellular carcinoma cells (Chen et al., 2009). In addition, the decrement of *MMP9* mRNA expression by U0126 and inhibitors of PI3K, wortmannin and LY294002, was also previously reported in ovarian and breast cancer cells (Thant et al., 2000; Reddy et al., 1999). Therefore, as we demonstrated, the inhibition of cell migration by RAD001 and U0126 was associated with the decrement of MMP2 and 9.

Yao and co-researchers recently reported that RAD001 administration was clinically effective for progression-free survival and the ratio of severe adverse events in progressive advanced pancreatic NETs in phase III clinical trials (Yao et al., 2011). However it is also true that mTOR inhibitors were associated with limitations caused by Akt and ERK activation in NET cells as reported in our present study. All of these findings including those of our present study suggest that the expression of activated Akt and ERK could be evaluated in surgical pathology specimens of NET cases prior to RAD001 treatment and the combined agent may be selected based upon the results of these evaluations. When Akt activation is detected in tumor cells using immunohistochemistry in biopsy specimens, somatostatin analogue may be administered because they were reported to inactivate Akt and to further stabilize symptoms (Arnold et al., 2000; Charland et al., 2001). The combined treatment of RAD001 with octreotide LAR (Novartis) has been evaluated in phase III clinical trial and its results demonstrated a

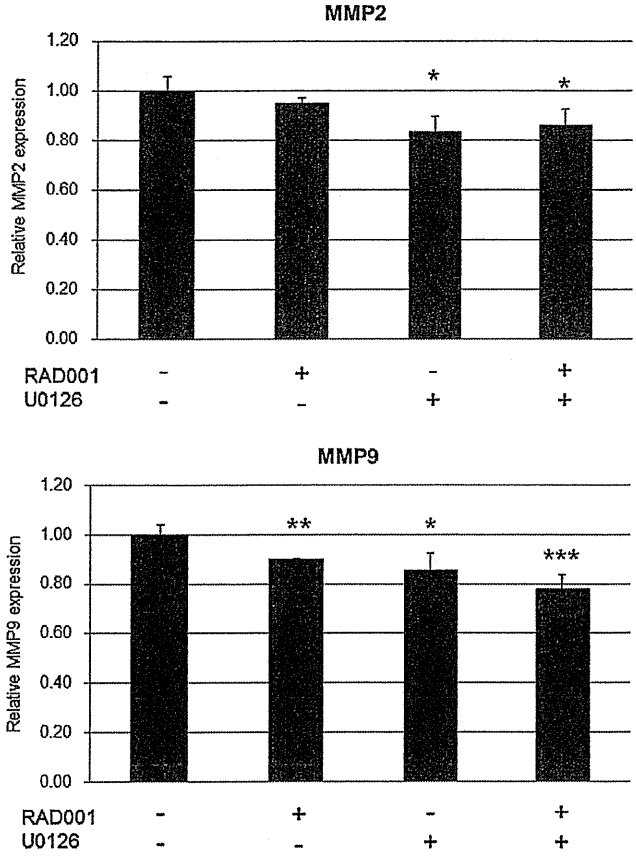

Fig. 6. Summary of mRNA levels of MMP2 and 9 in NCI-H727 when RAD001 and/or U0126 were treated. 100 nM of RAD001 and 1 μM of U0126 were respectively or simultaneously administered for 12 h and the expression levels of *MMP2* and *9* mRNA were evaluated. These experiments were performed in triplicate. $^{*}P < 0.05$, $^{**}P < 0.01$ and $^{***}P < 0.001$, compared with control group (Student *t* test).

significant clinical improvement in advanced NET patients (Pavel et al., 2011). Regarding Ras–Raf–MEK–ERK pathway, a MEK or a Raf inhibitor may be combined with an mTOR inhibitor (Hjelmeland et al., 2007). It is true that MEK or Raf inhibitors have not yet been clinically applied in any tumors but the development of the combined therapy has been expected. In addition, the effects detected in our present study may be also detected in other types of malignancies and the correlation of the findings obtained with neuroendocrine features of the tumors cells, that is, the synthesis and secretion of peptide hormones needs to be clarified by further investigations.

In summary, we firstly demonstrated the synergistic suppression of cell proliferation and invasive properties in the dual inhibition of mTOR and MEK in NET cell lines by suppressing the compensatory induction or activation of the pathway caused by suppression of mTOR or MEK signaling pathways. In our previous study, mTOR or ERK activation was detected in 63.5% and 34.6% of NET cases, respectively (Iida et al., 2010), and combined treatment may be effective when applied to the patients with NET.

Acknowledgements

We appreciate Novartis Oncology for supplying RAD001 for our analysis. We appreciate Miki Mori and Erina Iwabuchi (Department of Pathology, Tohoku University School of Medicine) for their skillful technical assistances despite the unprecedented enormous damages inflicted upon Tohoku University, Sendai, Japan by March 11th earthquake, which interrupted this study.

References

Amato, R.J., Jac, J., Giessinger, S., Saxena, S., Willis, J.P., 2009. A phase 2 study with a daily regimen of the oral mTOR inhibitor RAD001 (everolimus) in patients with metastatic clear cell renal cell cancer. Cancer 115, 2438–2446.

Arnold, R., Simon, B., Wied, M., 2000. Treatment of neuroendocrine GEP tumours with somatostatin analogues. Digestion 62, 84–91.

Bjornsti, M.A., Houghton, P.J., 2004. The TOR pathway: a target for cancer therapy. Nat. Rev. Cancer 4, 335–348.

Carracedo, A., Ma, L., Teruya-Feldstein, J., Rojo, F., Salmena, L., Alimonti, A., Egia, A., Sasaki, A.T., Thomas, G., Kozma, S.C., Papa, A., Nardella, C., Cantley, L.C., Baselga, J., Pandolfi, P.P., 2008. Inhibition of mTORC1 leads to MAPK pathway activation through a PI3K-dependent feedback loop in human cancer. J. Clin. Invest. 118, 3065–3074.

Chan, H.Y., Grossman, A.B., Bukowski, R.M., 2010. Everolimus in the treatment of renal cell carcinoma and neuroendocrine tumors. Adv. Ther. 27, 495–511.

Chang, Q., Chapman, M.S., Miner, J.N., Hedley, D.W., 2010. Antitumour activity of a potent MEK inhibitor RDEA110/BAY 869766 combined with rapamycin in human orthotopic primary pancreatic cancer xenograft. BMC Cancer 10, 515–526.

Charland, S., Boucher, M.J., Houde, M., Rivard, N., 2001. Somatostatin inhibits Akt phosphorylation and cell cycle entry, but not p42/p44 mitogen-activated protein (MAP) kinase activation in normal and tumoral pancreatic acinar cells. Endocrinology 142, 121–128.

Chen, J.S., Wang, Q., Fu, X.H., Huang, X.H., Chen, X.L., Cao, L.Q., Chen, L.Z., Tan, H.X., Li, W., Bi, J., Zhang, L.J., 2009. Involvement of PI3K/PTEN/AKT/mTOR pathway in invasion and metastasis in hepatocellular carcinoma: association with MMP-9. Hepatol. Res. 39, 177–186.

Chou, T.C., 2006. Theoretical basis, experimental design, and computerized simulation of synergism and antagonism in drug combination studies. Pharmacol. Rev. 58, 621–681.

Chou, T.C., 2010. Drug combination studies and their synergy quantification using the Chou-Talalay method. Cancer Res. 70, 440–446.

Chou, T.C., Talalay, P., 1984. Quantitative analysis of dose-effect relationships: the combined effects of multiple drugs or enzyme inhibitors. Adv. Enzyme Regul. 22, 27–55.

Ciuffreda, L., Di Sanza, C., Incani, U.C., Milella, M., 2010. The mTOR pathway: a new target in cancer therapy. Curr. Cancer Drug Targets 10, 484–495.

Duran, I., Kortmansky, J., Singh, D., Hirte, H., Kocha, W., Goss, G., Le, L., Oza, A., Nicklee, T., Ho, J., Birle, D., Pond, G.R., Arboine, D., Dancey, J., Aviel-Ronen, S., Tsao, M.S., Hedley, D., Siu, L.L., 2006. A phase II clinical and pharmacodynamic study of temsirolimus in advanced neuroendocrine carcinomas. Br. J. Cancer 95, 1148–1154.

Grozinsky-Glasberg, S., Franchi, G., Teng, M., Leontiou, C.A., Ribeiro de Oliveira, A., Dalino Jr., P., Salahuddin, N., Korbonits, M., Grossman, A.B., 2008. Octreotide and the mTOR inhibitor RAD001 (everolimus) block proliferation and interact with the Akt-mTOR-p70S6K pathway in a neuro-endocrine tumour cell line. Neuroendocrinology 87, 168–181.

Hartley, D., Cooper, G.M., 2002. Role of mTOR in the degradation of IRS-1: regulation of PP2A activity. J. Cell Biochem. 85, 304–314.

Herbert, T.P., Tee, A.R., Proud, C.G., 2002. The extracellular signal-regulated kinase pathway regulates the phosphorylation of 4E-BP1 at multiple sites. J. Biol. Chem. 277, 11591–11596.

Hess, G., Herbrecht, R., Romaguera, J., Verhoef, G., Crump, M., Gisselbrecht, C., Laurell, A., Offner, F., Strahs, A., Berkenblit, A., Hanushevsky, O., Clancy, J., Hewes, B., Moore, L., Coiffier, B., 2009. Phase III study to evaluate temsirolimus compared with investigator's choice therapy for the treatment of relapsed or refractory mantle cell lymphoma. J. Clin. Oncol. 27, 3822–3829.

Hjelmeland, A.B., Lattimore, K.P., Fee, B.E., Shi, Q., Wickman, S., Keir, S.T., Hjelmeland, M.D., Batt, D., Bigner, D.D., Friedman, H.S., Rich, J.N., 2007. The combination of novel low molecular weight inhibitors of RAF (LBT613) and target of rapamycin (RAD001) decreases glioma proliferation and invasion. Mol. Cancer Ther. 6, 2449–2457.

Hoshino, R., Tanimura, S., Watanabe, K., Kataoka, T., Kohno, M., 2001. Blockade of the extracellular signal-regulated kinase pathway induces marked G1 cell cycle arrest and apoptosis in tumor cells in which the pathway is constitutively activated upregulation of p27Kip1. J. Biol. Chem. 276, 2686–2692.

Iida, S., Miki, Y., Ono, K., Akahira, J., Suzuki, T., Ishida, K., Watanabe, M., Sasano, H., 2010. Novel classification based on immunohistochemistry combined with hierarchical clustering analysis in non-functioning neuroendocrine tumor patients. Cancer Sci. 101, 2278–2285.

Jayaraman, T., Marks, A.R., 1993. Rapamycin-FKBP12 blocks proliferation, induces differentiation, and inhibits cdc2 kinase activity in a myogenic cell line. J. Biol. Chem. 268, 25385–25388.

Jin, N., Jiang, T., Rosen, D.M., Nelkin, B.D., Ball, D.W., 2009. Dual inhibition of mitogen-activated protein kinase kinase and mammalian target of rapamycin in differentiated and anaplastic thyroid cancer. J. Clin. Endocrinol. Metab. 94, 4107–4112.

Johannessen, C.M., Boehm, J.S., Kim, S.Y., Thomas, S.R., Wardwell, L., Johnson, L.A., Emery, C.M., Stransky, N., Cogdill, A.P., Barretina, J., Caponigro, G., Hieronymus, H., Murray, R.R., Salehi-Ashtiani, K., Hill, D.E., Vidal, M., Zhao, J.J., Yang, X., Alkan, O., Kim, S., Harris, J.L., Wilson, C.J., Myer, V.E., Finan, P.M., Root, D.E., Roberts, T.M., Golub, T., Flaherty, K.T., Dummer, R., Weber, B.L., Sellers, W.R., Schlegel, R., Wargo, J.A., Hahn, W.C., Garraway, L.A., 2010. COT drives resistance to RAF inhibition through MAP kinase pathway reactivation. Nature 468, 968–973.

Kikade, C.W., Castillo-Martin, M., Puzio-Kuter, A., Yan, J., Foster, T.H., Gao, H., Sun, Y., Ouyang, X., Gerald, W.L., Cordon-Cardo, C., Abate-Shen, C., 2008. Targeting AKT/mTOR and ERK/MAPK signaling inhibits hormone-refractory prostate cancer in a preclinical mouse model. J. Clin. Invest. 118, 3051–3064.

Lasithiotakis, K.G., Sinnberg, T.W., Schittek, B., Flaherty, K.T., Kulms, D., Maczey, E., Garbe, C., Meier, F.E., 2008. Combined inhibition of MAPK and mTOR signaling inhibits growth, induces cell death, and abrogates invasive growth of melanoma cells. J. Invest. Dermatol. 128, 2013–2023.

Lavoie, J.N., L'Allemain, G.L., Brunet, A., Müller, R., Pouysségur, J., 1996. Cyclin D1 expression is regulated positively by the p42/44MAPK and negatively by the p38/HOGMAPK pathway. J. Biol. Chem. 271, 20608–20616.

Liang, C.C., Park, A.Y., Guan, J.L., 2007. *In vitro* scratch assay: a convenient and inexpensive method for analysis of cell migration *in vitro*. Nat. Protoc. 2, 329–333.

Loewith, R., Jacinto, E., Wullschleger, S., Lorberg, A., Crespo, J.L., Bonenfant, D., Oppliger, W., Jenoe, P., Hall, M.N., 2002. Two TOR complexes, only one of which is rapamycin sensitive, have distinct roles in cell growth control. Mol. Cell 10, 457–468.

Meng, J., Peng, H., Dai, B., Guo, W., Wang, L., Ji, L., Minna, J.D., Chresta, C.M., Smith, P.D., Fang, B., Roth, J.A., 2009. High level of AKT activity is associated with resistance to MEK inhibitor AZD6244 (ARRY-142886). Cancer Biol. Ther. 21, 2073–2080.

Mi, R., Ma, J., Zhang, D., Li, L., Zhang, H., 2009. Efficacy of combined inhibition of mTOR and ERK/MAPK pathways in treating a tuberous sclerosis complex cell model. J. Genet. Genomics 36, 355–361.

Moreno, A., Akcakanat, A., Munsell, M.F., Soni, A., Yao, J.C., Meric-Bernstam, F., 2008. Antitumor activity of rapamycin and octreotide as single agents or in combination in neuroendocrine tumors. Endocr. Relat. Cancer 15, 257–266.

Nazarian, R., Shi, H., Wang, Q., Kong, X., Koya, R.C., Lee, H., Chen, Z., Lee, M.K., Attar, N., Sazegar, H., Chondon, T., Nelson, S.F., McArthur, G., Sosman, J.A., Ribas, A., Lo, R.S., 2010. Melanomas acquire resistance to B-RAF(V600E) inhibition by RTK or N-RAS upregulation. Nature 468, 973–979.

O'Reilly, K.E., Rojo, F., She, Q.B., Solit, D., Mills, G.B., Smith, D., Lane, H., Hofmann, F., Hicklin, D.J., Ludwig, D.L., Baselga, J., Rosen, N., 2006. MTOR inhibition induces upstream receptor tyrosine kinase signaling and activates Akt. Cancer Res. 66, 1500–1508.

Pavel, M., Peeters, M., Hörsch, D., Van Cutsem, E., Öberg, K., Jehl, V., Klimovsky, J., Yao, J., 2011. Everilumus + Octreotide LAR vs placebo + Octreotide LAR in patients with advanced neuroendocrine tumors (NET): Updated results of a randomized double-blind, placebo-controlled, multicenter phase III trial (RADIANT-2). The 8th Annual ENETS Conferences, C86.

Pouysségur, J., Dayan, F., Mazure, N., 2006. Hypoxia signaling in cancer and approaches to enforce tumour regression. Nature 441, 437–443.

Quinn, L.A., Moore, G.E., Morgan, R.T., Woods, L.K., 1979. Cell lines from human colon carcinoma with unusual cell products, double minutes, and homogeneously staining regions. Cancer Res. 39, 4914–4924.

Reddy, K.B., Krueger, J.S., Kondapaka, S.B., Diglio, C.A., 1999. Mitogen-activated protein kinase (MAPK) regulates the expression of progelatinase B (MMP-9) in breast epithelial cells. Int. J. Cancer 82, 268–273.

Reidy, D.L., Tang, L.H., Saltz, L.B., 2009. Treatment of advanced disease in patients with well-differentiated neuroendocrine tumors. Nat. Clin. Pract. 6, 143–152.

Sunayama, J., Matsuda, K., Sato, A., Tachibana, K., Suzuki, K., Narita, Y., Shibui, S., Sakurada, K., Kayama, T., Tomiyama, A., Kitanaka, C., 2010. Crosstalk between the PI3K/mTOR and MEK/ERK pathways involved in the maintenance of self-renewal and tumorigenecity of glioblastoma stem-like cells. Stem Cells 28, 1930–1939.

Thant, A.A., Nawa, A., Kikkawa, F., Ichigotani, Y., Zhang, Y., Sein, T.T., Amin, A.R., Hamaguchi, M., 2000. Fibronectin activates matrix metalloproteinase-9 secretion via the MEK1-MAPK and the PI3K-Akt pathways in ovarian cancer cells. Clin. Exp. Metastasis 18, 423–428.

Theodoropoulou, M., Zhang, J., Laupheimer, S., Paez-Pereda, M., Erneux, C., Florio, T., Pagotto, U., Stalla, G.K., 2006. Octreotide, a somatostatin analogue, mediates its antiproliferative action in pituitary tumor cells by altering phosphatidylinositol 3-kinase signaling and inducing Zac1 expression. Cancer Res. 66, 1576–1582.

Thomson, A.W., Turnauist, H.R., Raimondi, G., 2009. Immunoregulatory functions of mTOR inhibition. Nat. Rev. Immunol. 9, 324–337.

Vilella-Bach, M., Nuzzi, P., Fang, Y., Chen, J., 1999. The FKBP12-rapamycin-binding domain is required for FKBP12-rapamycin-associated protein kinase activity and G_1 progression. J. Biol. Chem. 274, 4266–4272.

von Wichert, G., Jehle, P.M., Hoeflich, A., Koschnick, S., Dralle, H., Wolf, E., Wiedenmann, B., Boehm, B.O., Adler, G., Seufferlein, T., 2000. Insulin-like growth factor-I is an autocrine regulator of chromogranin A secretion and growth in human neuroendocrine tumor cell. Cancer Res. 60, 4573–4581.

Wang, L., Gout, I., Proud, C.G., 2001. Cross-talk between the ERK and p70 S6 kinase (S6K) signaling pathways. J. Biol. Chem. 276, 32670–32677.

Wang, X., Hawk, N., Yue, P., Kauh, J., Ramalingam, S.S., Fu, H., Khuri, F.R., Sun, S.Y., 2008. Overcoming mTOR inhibition-induced paradoxical activation of survival signaling pathways enhances mTOR inhibitors' anticancer efficacy. Cancer Biol. Ther. 7, 1952–1958.

Wullschleger, S., Loewith, R., Hall, M.N., 2006. TOR signaling in growth and metabolism. Cell 124, 471–484.

Yao, J.C., Phan, A.T., Chang, D.Z., Wolff, R.A., Hess, K., Gupta, S., Jacobs, C., Mares; J.E., Landgraf, A.N., Rashid, A., Meric-Bernstam, F., 2008. Efficacy of RAD001 (everolimus) and octreotide LAR in advanced low- to intermediate-grade neuroendocrine tumors: results of a phase II study. J. Clin. Oncol. 26, 4311–4318.

Yao, J.C., Shah, M.H., Ito, T., Bohas, C.L., Wolim, E.M., Van Cutsem, E., Hobday, T.J., Okusaka, T., Capdevila, J., de Vries, E.G., Tomassetti, P., Pavel, M.E., Hoosen, S., Haas, T., Lincy, J., Lebwohl, D., Öberg, K., 2011. RAD001 in Advanced Neuroendocrine tumors, third trial (RADIANT-3) study group. Everolimus for advanced pancreatic neuroendocrine tumors. N. Engl. J. Med. 10, 514–523.

Yu, K., Toral-Barza, L., Discafani, C., Zhang, W.G., Skotnicki, J., Frost, P., Gibbons, J.J., 2001. MTOR, a novel target in breast cancer: the effect of CCI-779, an mTOR inhibitor, in preclinical models of breast cancer. Endocr. Relat. Cancer 8, 249–258.

Zhang, D., Bar-Eli, M., Meloche, S., Brodt, P., 2004. Dual regulation of MMP-2 expression by the type 1 insulin-like growth factor receptor: the phosphatidylinositol 3-kinase/Akt and Raf/ERK pathways transmit opposing signals. J. Biol. Chem. 279, 19683–19690.

Zhang, H., Bajraszewski, N., Wu, E., Wang, H., Mosenman, A.P., Dabora, S.L., Griffin, J.D., Kwiatkowski, D.J., 2007. PDGFRs are critical for PI3K/Akt activation and negatively regulated by mTOR. J. Clin. Invest. 117, 730–738.

Zitzmann, K., von Rüden, J., Brand, S., Göke, B., Lichtl, J., Spöttl, G., Auernhammer, C.J., 2010. Compensatory activation of Akt in response to mTOR and Raf inhibitors – a rationale for dual-targeted therapy approaches in neuroendocrine tumor disease. Cancer Lett. 295, 100–109.

Zutzmann, K., De Toni, E.N., Brand, S., Göke, B., Meinecke, J., Spöttl, G., Meter, H.H., Auernhammer, C.J., 2007. The novel mTOR inhibitor RAD001 (Everolimus) induces antiproliferative effects in human pancreatic neuroendocrine tumor cells. Neuroendocrinology 85, 54–60.

JJCO Japanese Journal of Clinical Oncology

Jpn J Clin Oncol 2012;42(3)168–174
doi:10.1093/jjco/hyr197
Advance Access Publication 4 January 2012

Breast Ultrasonographic and Histopathological Characteristics Without Any Mammographic Abnormalities

Kentaro Tamaki[1,2,3,*], Takanori Ishida[2], Minoru Miyashita[2], Masakazu Amari[2], Noriaki Ohuchi[2], Yoshihiko Kamada[1], Kano Uehara[1], Nobumitsu Tamaki[1] and Hironobu Sasano[3]

[1]Department of Breast Surgery, Nahanishi Clinic, Okinawa, [2]Department of Surgical Oncology, Tohoku University Graduate School of Medicine and [3]Department of Pathology, Tohoku University Hospital, Miyagi, Japan

*For reprints and all correspondence: Kentaro Tamaki, 1-1 Seiryo-machi, Aoba-ku, Sendai, Miyagi 980-8574, Japan. E-mail: nahanisikenta@yahoo.co.jp

Received October 13, 2011; accepted December 13, 2011

Objective: We evaluated ultrasonographic findings and the corresponding histopathological characteristics of breast cancer patients with Breast Imaging Reporting and Data System (BI-RADS) category 1 mammogram.
Methods: We retrospectively reviewed the ultrasonographic findings and the corresponding histopathological features of 45 breast cancer patients with BI-RADS category 1 mammogram and 537 controls with mammographic abnormalities. We evaluated the ultrasonographic findings including mass shape, periphery, internal and posterior echo pattern, interruption of mammary borders and the distribution of low-echoic lesions, and the corresponding histopathological characteristics including histological classification, hormone receptor and human epidermal growth factor receptor 2 status of invasive ductal carcinoma and ductal carcinoma *in situ*, histological grade, mitotic counts and lymphovascular invasion in individual cases of BI-RADS category 1 mammograms and compared with those of the control group.
Results: The ultrasonographic characteristics of the BI-RADS category 1 group were characterized by a higher ratio of round shape ($P < 0.001$), non-spiculated periphery ($P = 0.021$), non-interruption of mammary borders ($P < 0.001$) and non-attenuation ($P = 0.011$) compared with the control group. A total of 52.6% of low-echoic lesions were associated with spotted distribution in the BI-RADS 1 group, whereas 25.8% of low-echoic lesions were associated with spotted distribution in the control group ($P = 0.012$). As for histopathological characteristics, there was a statistically higher ratio of triple-negative subtype ($P = 0.021$), and this particular tendency was detected in histological grade 3 in the BI-RADS category 1 group ($P = 0.094$).
Conclusion: We evaluated ultrasonographic findings and the corresponding histopathological characteristics for BI-RADS category 1 mammograms and noted significant differences among these findings in this study. Evaluation of these ultrasonographic and histopathological characteristics may provide a more accurate ultrasonographic screening system for breast cancer in Japanese women.

Key words: breast US – BI-RADS category 1 mammogram – histopathological characteristics

INTRODUCTION

The incidence of breast cancer has increased worldwide, which is partly considered to be due to mass screening programs resulting in the discovery of clinically occult or early breast lesions (1). Early clinical detection of breast cancer through screening has therefore led to the detection of the tumor at a relatively earlier clinical stage. The effectiveness of screening mammography on reduction in mortality by breast cancer has been well established in both Western countries and Japan (2). Mammography has thus become the gold standard for

detecting breast disorders. Therefore, it has become very important to increase the rate of mammographic screening among the general public toward reducing the breast cancer mortality. However, it is also true that 7.2% of the malignant cases were associated with no mammographic abnormalities (3). In addition, the malignant ratio of 20, 30 and 40 years without mammographic abnormalities was statistically higher than the ratio of the other age groups (3). Ultrasonography (US) has been in general proposed to prove much more effective in the detection of breast cancer if the patient is young, has dense breast or their detected masses are small (4–6). Therefore, it has become very important to improve the quality of US diagnoses.

The effectiveness of ultrasound screening for women aged 40 years has been evaluated in detecting and reducing mortality of the breast cancer in Japan in order to complement this particular pitfall of mammography (7). This study named J-START (The Japan Strategic Anti-cancer Randomized Trial) evaluates the effectiveness of screening mammography with US breast cancer screening compared with mammography alone in 40 years, with a design to study 50 000 women with mammography and US and 50 000 controls with mammography only (7). The participants are scheduled to take a second-round screening with the same modality 2 years onwards (7). The primary endpoints are sensitivity and specificity, and the secondary endpoint as the rate of advanced breast cancer (7). Whether or not breast US screening is adopted in the future large-scale screening therefore largely depends on the results of this research. Considerable efforts will be required to successfully carry out this massive undertaking done in Japanese population.

Strict or rigorous conformity to high quality of interpretation of US finding among those involved in this screening is therefore mandatory for the very success of an US diagnosis in such a large scale. We previously examined the correlation between US findings and the corresponding histopathological features in breast disorders in our previous study (6). There have been relatively few reported studies on assessing US performance and its resolution without any mammographic abnormalities (8). Therefore, in this study, we evaluated US findings and the corresponding histopathological characteristics for breast cancer patients with Breast Imaging Reporting and Data System (BI-RADS) (9) category 1 mammogram.

PATIENTS AND METHODS

Patients

We retrospectively reviewed the US findings and their corresponding histopathological features of 45 breast cancer patients with BI-RADS category 1 mammogram and 537 controls with mammographic abnormalities. The patients underwent needle biopsies or surgical resection at the Tohoku University Hospital from January 2006 to December 2010. We received informed consents from all the patients and the protocol for this study was approved by the Ethics Committee at Tohoku University Graduate School of Medicine.

Imaging Devices and Breast Tissue Specimens

The US examinations were assessed by one of the experienced eight breast specialists in Tohoku University Hospital. The consensus meeting of US was held for 1 whole week in order to standardize the US examination among these eight doctors. In addition, two of them independently evaluated the US findings in a retrospective manner, without the knowledge of clinical and histopathological information of individual patients. All US evaluations were carried out using Aloka SSD 3500 and ProSound α7 (Aloka Co., Tokyo, Japan) with a 10 MHz transducer.

We stained the corresponding tissue slides of the cases using hematoxylin–eosin (H&E) and immunohistochemistry for estrogen receptor (ER) and human epidermal growth factor receptor 2 (HER2). Surgical specimens had been fixed in 10% formaldehyde solution, cut into serial 5 mm-thick slices, embedded in paraffin, cut into 4 μm-thick sections and placed on the glue-coated glass slides. We employed the avidin–streptavidin immunoperoxidase method using the clone 6F11 antibody (Ventana, Tucson, AZ, USA) in automated immunostainer (Benchmark System; Ventana). A standardized immunohistochemistry kit (HercepTest for Immunoenzymatic Staining; Dako, Copenhagen, Denmark) was used for HER2 staining. Histopathological slides were reviewed by two pathologists independently without the knowledge of clinical information. Olympus (Tokyo, Japan) BX50 and 20× objectives were used for the analyses.

Imaging and Histopathological Analyses

Two or more hardcopy transverse and sagittal plane images of breast lesions were analyzed in this study. We recorded tumor shape, periphery, internal and lateral echo pattern, interruption of mammary borders and the distribution of low-echoic lesions, according to the BI-RADS sonographic classification (9) and the Japan Association of Breast and Thyroid Sonology (JABTS) breast sonographic classification (10). Tumor shape was tentatively classified into round, oval, lobular and irregular (9,10). Periphery was tentatively classified into circumscribed, obscured, indistinct and spiculated (9,10). Internal echo was classified into low and heterogeneity or high (9,10). Lateral echo was also classified into accentuation, no change and attenuation (9,10). Interruption of mammary borders was classified into interruption, indeterminate and no (9,10). Distribution of low-echoic lesions was classified into spotted and segmental (9,10) (Fig. 1).

Two of the experienced pathologists independently evaluated surgical pathology specimens, respectively. Histopathological evaluations were based on World Health Organization (WHO) histological classification of tumor of the breast (11) and Rosen's breast pathology (12). ER was determined by nuclear staining graded from 0 to 8 using the Allred score, and ER positivity was Grade 3 or more (13). With regard to HER2 evaluation, membranous staining was graded as the following: score 0–1+, 2+ and 3+ (14).

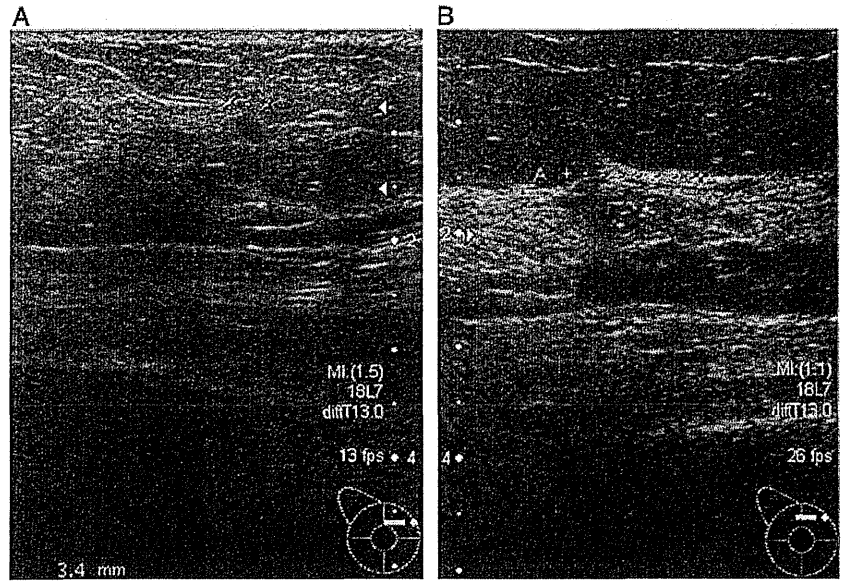

Figure 1. Representative illustrations of the distribution of low-echoic lesions. (A) Spotted and (B) segmental.

Scoring of 2+ was added fluorescence *in situ* hybridization (FISH) that was used to calculate the gene copy ratio of HER2-to-CEP17 (the PathVysion HER2 DNA Probe Kit; Abbott, Chicago, IL, USA). Positive is defined as either HER2:CEP17 signal ratio (FISH score) >2.2 (14). Histological grades and mitotic counts were assessed according to the criteria of Elston and Ellis (15). Van Nuys classifications were also assessed for ductal carcinoma *in situ* and invasive ductal carcinoma (IDC) with predominant intraductal components cases (16,17). We also identified the presence or absence of lymphovascular invasion according to the Rosen's Breast Pathology (12).

At first, we examined the differences of the patients' characteristics between these two groups including the distribution of age, menopausal status, past history of the benign proliferative disease, background of detection, clinical stage, breast density of mammography according to the BI-RADS lexicon (9) and surgical strategy as the breast-conserving ratio. We evaluated the US findings including mass shape, periphery, internal and posterior echo pattern, interruption of mammary borders and the distribution of low-echoic lesions and compared them with histopathological characteristics including histological classification, hormone receptor and HER2 status of IDC, tumor size confirmed by histopathology, histological grade, mitotic counts and lymphovascular invasion of BI-RADS category 1 mammograms. We then compared these findings with those of control group patients.

Statistical Analyses

Statistical analyses were performed using StatMate III for Windows ver. 3.18 (ATMS, Tokyo, Japan). The results were considered significant at $P < 0.05$.

RESULTS

The Details of Both BI-RADS 1 and Control Groups

Table 1 summarizes the difference in the patients' characteristics including the distribution of age, menopausal status, past history of the benign proliferative disease, background of detection, clinical stage, breast density of mammography and surgical strategy. The median ages of the study group and the control group were 48 years (range, 32–84) and 56 years (range, 26–88), respectively ($P = 0.047$). There was a statistically significant higher ratio of Stages 0 and I, heterogeneously and extremely dense, and conserving surgery in the BI-RADS 1 group ($P < 0.001$, <0.001 and 0.002, respectively). However, there was a statistically significant lower ratio of menopause and self-palpation in the BI-RADS 1 group ($P < 0.001$, respectively; Table 1).

Table 1. The details of patients

	BI-RADS 1	Control	*P* value	Odds ratio
Age	48 (32–84)	56 (26–88)	0.047	—
Menopausal ratio	37.8%	63.4%	<0.001	0.31
Benign proliferative disease	2.2%	9.5%	NS	2.34
Cause of detection (self-palpation ratio)	24.4%	59.4%	<0.001	0.22
Stage (Stages 0 and I)	93.3%	66.4%	<0.001	7.08
Heterogeneously and extremely dense ratio	91.1%	39.1%	<0.001	15.97
Surgical strategy (conserving ratio)	95.6%	74.6%	0.002	7.82

The Ratios of Mass Cases and the Tumor Size

Twenty-six out of the 45 were US mass cases in the BI-RADS 1 group and 370 out of the 490 were US mass cases in the control group. There was a statistically significant difference between the BI-RADS 1 and control groups ($P = 0.003$). The US tumor size of BI-RADS 1 and control groups was 12.1 mm (range, 3.2–24.9 mm) and 18.5 mm (range, 6.5–150 mm) with statistically significant differences ($P < 0.001$).

Evaluation of the US Characteristics

Figure 2 summarizes the results of the numbers and ratios of mass shape (Fig. 2A), periphery (Fig. 2B), internal echo pattern (Fig. 2C), lateral echo pattern (Fig. 2D) and interruption of mammary borders (Fig. 2E) of the BI-RADS 1 and control groups. There were statistically higher ratios of round mass shape ($P < 0.001$), no change of lateral echo pattern ($P = 0.028$) and no or indeterminate interruption of mammary borders ($P < 0.001$) in the BI-RADS 1 group. There were statistically lower ratios of spiculated periphery ($P = 0.021$), attenuation of lateral echo pattern ($P = 0.011$) and interruption of mammary borders ($P < 0.001$) in the BI-RADS 1 group. Figure 3 summarizes the results of the numbers and ratios of distribution of low-echoic lesions. There were statistically higher ratios of spotted distribution and lower cases of segmental distribution in the BI-RADS 1 group than in the control group ($P = 0.012$).

Evaluation of the Corresponding Histopathological Characteristics

Figure 4 summarizes the results of the numbers and ratios of results classified by histological subtypes (Fig. 4A), hormone receptor and HER2 expression of IDC (Fig. 4B), tumor size of the invasive lesion as confirmed by the histopathological examination (Fig. 4C), histological grade (Fig. 4D), mitotic counts (Fig. 4E) and lymphovascular invasion (Fig. 4F). There was statistically higher ratios of triple-negative subtype, smaller tumor size and lower case of lymphovascular invasion in the BI-RADS 1 group ($P = 0.021$, $P < 0.001$ and $P = 0.012$, respectively) compared with the control group. In addition, a higher ratio of histological grade 3 was detected in the BI-RADS 1 group but this difference did not reach the statistical significance ($P = 0.094$).

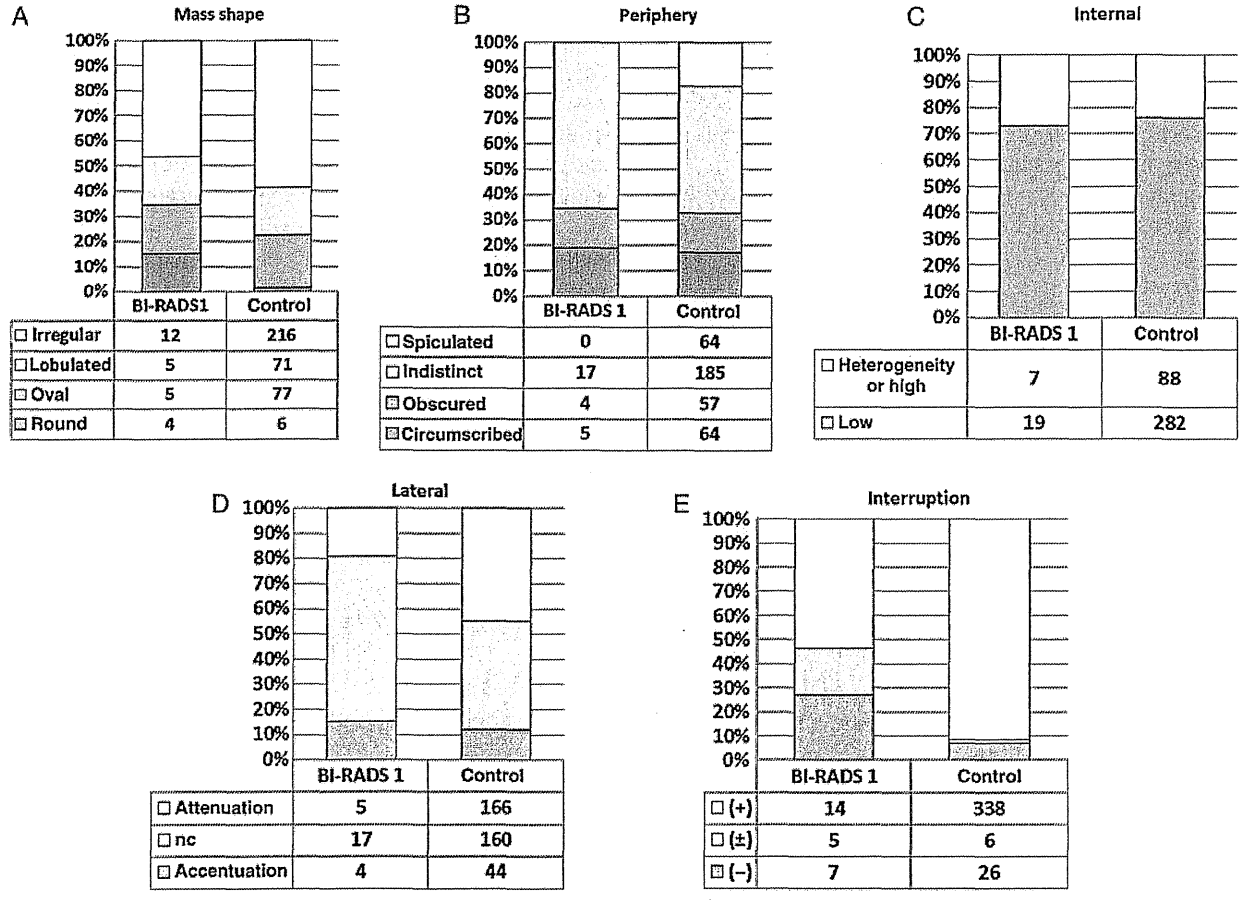

Figure 2. The US characteristics of BI-RADS category 1 and control groups. (A) Mass shape, (B) periphery, (C) internal echo pattern, (D) lateral echo pattern and (E) interruption of mammary borders.

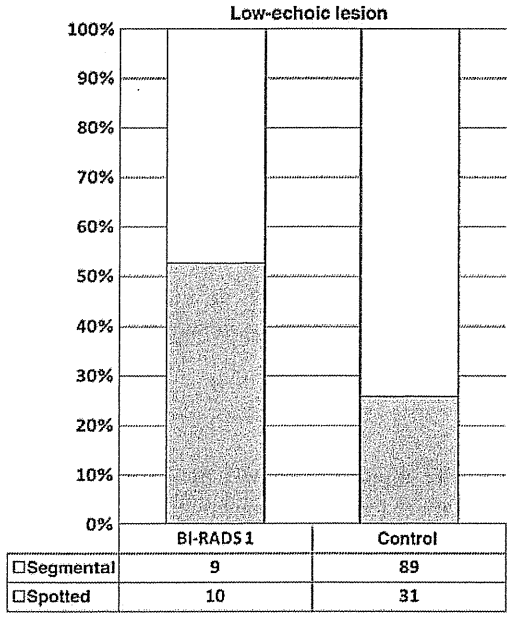

Figure 3. The distribution of low-echoic lesions of BI-RADS category 1 and control groups.

DISCUSSION

Mammography has been considered a gold standard for breast cancer screening system. However, US screening combined with mammography may have the potential to become one of the useful screening systems to decrease breast cancer mortality according to the results of the J-START trial (7). Therefore, strict or rigorous conformation to high quality of interpreting the US findings is required or mandatory for the future success of an US diagnosis especially at the level of mass screening. Our present study is the first study to focus upon incremental detection of breast cancer by US in asymptomatic women with mammography-negative breasts, and focused on the US findings and the corresponding histopathological characteristics of the cases with BI-RADS category 1 mammograms.

US detected cancers are in general smaller than those identified with mammography. Results of our present study demonstrated that the BI-RADS category 1 group was associated with a statistically higher ratio of low-echoic lesions than the control group. In addition, 52.6% of low-echoic lesions demonstrated spotted distribution in the BI-RADS 1 group, whereas 25.8% of low-echoic lesions spotted

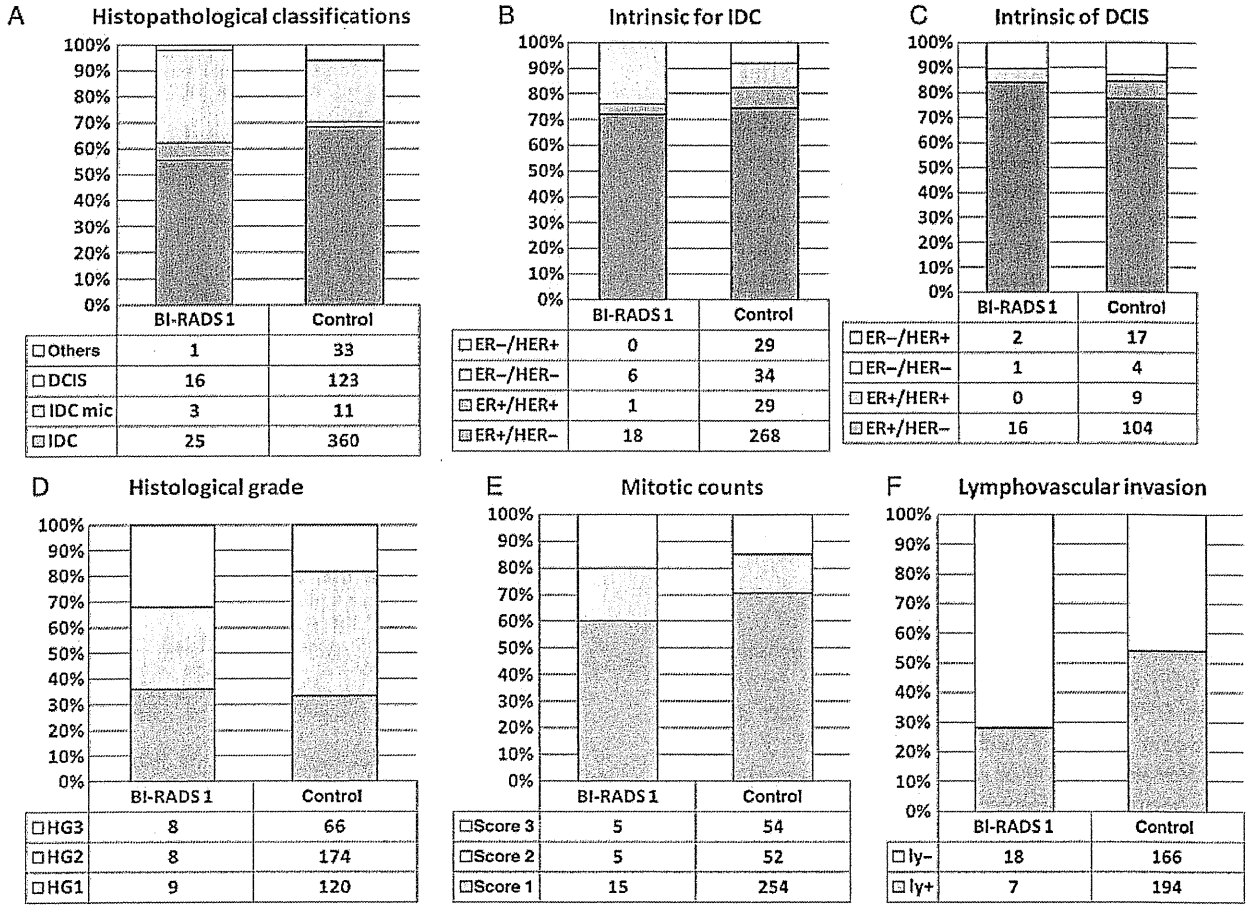

Figure 4. The histopathological characteristics of BI-RADS category 1 and control groups. (A) Histological classification, (B) hormone receptor and human epidermal growth factor receptor 2 expression of invasive ductal carcinoma, (C) tumor size of the invasive lesion, (D) histological grade, (E) mitotic counts and (F) lymphovascular invasion.

distribution in the control group. A low-echoic lesion with spotted distribution is therefore considered one of the predicting factors of malignancy in the BI-RADS category 1 group. In addition, the tumor size of the BI-RADS 1 group was smaller, and the detected masses were characterized by a higher ratio of round shape, non-spiculated periphery, non-interruption of mammary borders and non-attenuation in the BI-RADS category 1 group. These results could be mainly affected by mammographic breast density. In addition, results of our present study also demonstrated that there was a statistically higher ratio of heterogeneously and extremely dense breast in the BI-RADS 1 group and the tumors with well-collagenized stromal reaction were also detected as architectural distortion or spiculation in dense breast mammogram. Therefore, mammographic breast density was reasonably postulated to influence characteristics of breast cancers with BI-RADS category 1. Results of previous studies demonstrated that the most breast cancer cases of BI-RADS category 1 were relatively hypoechoic within a background of hyperechoic fibroglandular tissue, which may make the lesions more conspicuous and detectable (18). However, it is also true that previous studies have not evaluated the US findings of BI-RADS category 1 cases and this is the first study demonstrating the US findings such as mass shape and periphery of BI-RADS category 1 cases. In addition, this is the first reported study to demonstrate histopathological characteristics of BI-RADS category 1 cases. The statistically higher ratio of triple-negative subtype was detected in BI-RADS category 1 cases, and histological grade 3 tended to be also higher in the BI-RADS category 1 group. Results above did indicate that the BI-RADS category 1 group was histologically characterized by a higher malignant level than those with mammographic abnormalities, but it awaits further investigations for clarification.

Previous study also demonstrated that earlier detection of breast cancer resulted in a decrement in mortality, which parallels the reduction in size distribution of cancers depicted and closely parallels the reduction in rates of node-positive breast cancer (19). Screening US also appears to detect many breast cancer cases at a smaller size and earlier stage compared with mammographic screening. In addition, in women with mammography dense breast, US was reported to be able to detect a substantially larger number of cancers with a supplemental cancer detection of 0.3–0.5% by US alone (18). Therefore, it is important to detect the US findings with the localized low-echoic lesion. In addition, among the BI-RADS category 1 group, particular attention should be paid to the US findings such as solidary differentiated masses such as oval or round shape and non-spiculated periphery because the corresponding histopathological features of the cases associated with these US findings above include a much higher ratio of triple-negative subtype and/or histological grade 3. Therefore, early detection of such solidary masses with triple-negative subtype and/or high histological grade by US may possibly contribute to the eventual reduction in breast cancer mortality.

We evaluated US findings and the corresponding histopathological characteristics for BI-RADS category 1 mammograms and noted significant differences among these findings in this study. Evaluation of these US and histopathological characteristics may provide a more accurate US screening system for Japanese women.

Acknowledgement

We thank Yayoi Takahashi, MT, for her excellent technical assistance for immunohistochemical staining.

Funding

This work was supported in part by a Grant-in Aid from 'Kurokawa Cancer Research Foundation'.

Conflict of interest statement

None declared.

References

1. Sutela A, Vanninen R, Sudah M, Berg M, Kiviniemi V, Rummukainen J, et al. Surgical specimen can be replaced by core samples in assessment of ER, PR and HER-2 for invasive breast cancer. *Acta Oncol* 2008;47:38–46.
2. Kawai M, Kuriyama S, Suzuki A, Nishino Y, Ishida T, Ohnuki K, et al. Effect of screening mammography on breast cancer survival in comparison to other detection methods: a retrospective cohort study. *Cancer Sci* 2009;100:1479–84.
3. Tamaki K, Sasano H, Miyashita M, Ishida T, Amari M, Ohuchi N, et al. A new mammographic classification: as a potential predictor of breast disorders for Asian women. 12th International St Gallen Breast Cancer Conference, St Gallen, Switzerland, 2011, SG-BCC2011-1204.
4. Osako T, Takahashi K, Iwase T, Iijima K, Miyagi Y, Nishimura S, et al. Diagnostic ultrasonography and mammography for invasive and noninvasive breast cancer in women aged 30–39 years. *Breast Cancer* 2007;14:229–33.
5. Crystal P, Strano SD, Shcharynski S, Koretz MJ. Using sonography to screen women with mammographically dense breasts. *Am J Roentgenol* 2003;181:177–82.
6. Tamaki K, Sasano H, Ishida T, Ishida K, Miyashita M, Takeda M, et al. The correlation between ultrasonographic findings and pathologic features in breast disorders. *Jpn J Clin Oncol* 2010;40:905–12.
7. Ohuchi N, Ishida T, Kawai M, Narikawa Y, Yamamoto S, Sobue T. Randomized controlled trial on effectiveness of ultrasonography screening for breast cancer in women aged 40–49 (J-START): research design. *Jpn J Clin Oncol* 2011;41:275–7.
8. Zanello PA, Robim AFC, Goncalves de Oliveira TM, Elias Junior J, Andrade JM, Monteiro CR, et al. Breast ultrasound diagnostic performance and outcomes for mass lesions using Breast Imaging Reporting and Data System category 0 mammogram. *Clinics* 2011;66:443–8.
9. American College of Radiology (ACR). *Breast Imaging Reporting and Data System (BI-RADS™)*. 4th edn. Reston, VA: American College of Radiology 2003.
10. Japan Association of Breast and Thyroid Sonography. *Guideline for Breast Ultrasound-Management and Diagnosis*. 2nd edn. Tokyo: Japanese 2008.
11. Tavassoli FA, Devilee P. *World Health Organization Classification of Tumors. Tumor of the Breast and Females Genital Organs*. Lyon: IARC Press 2003.
12. Rosen PP. *Rosen's Breast Pathology*. 3rd edn. Philadelphia, PA: Lippincott Williams & Wilkins 2009.

13. Allred DC, Harvey JM, Berardo M, Clark GM. Prognostic and predictive factors in breast cancer by immunohistochemical analysis. *Mod Pathol* 1998;11:155–68.
14. Wolff AC, Hammond ME, Schwartz JN, Hagerty KL, Allred DC, Cote RJ, et al. American society of clinical oncology/college of American pathologists guideline recommendations for human epidermal growth factor receptor 2 testing in breast cancer. *J Clin Oncol* 2007;25:118–45.
15. Elston CW, Ellis IO. Pathological prognostic factors in breast cancer. I. The value of histopathological grade in breast cancer: experience from a large study with long-term follow-up. *Histopathology* 1991;19:403–10.
16. Silverstein MJ. Prognostic classification of breast ductal carcinoma in situ. *Lancet* 1995;345:1154–7.
17. Tamaki K, Moriya T, Sato Y, Ishida T, Maruo Y, Yoshinaga K, et al. Vasohibin-1 in human breast carcinoma: a potential negative feedback regulator of angiogenesis. *Cancer Sci* 2009;100:88–94.
18. Youk JH, Kim EK. Supplementary screening sonography in mammographically dense breast: pros and cons. *Korean J Radiol* 2010;11:589–93.
19. Berg WA. Beyond standard mammographic screening: mammography at age extremes, ultrasound, and MR imaging. *Radiol Clin North Am* 2007;45:895–906.

Cancer Science
The official journal of the Japanese Cancer Association JCA

Nucleobindin 2 in human breast carcinoma as a potent prognostic factor

Shiho Suzuki,[1] Kiyoshi Takagi,[1,5] Yasuhiro Miki,[2] Yoshiaki Onodera,[2] Jun-ichi Akahira,[2] Akiko Ebata,[2,3] Takanori Ishida,[3] Mika Watanabe,[4] Hironobu Sasano[2,4] and Takashi Suzuki[1]

Departments of [1]Pathology and Histotechnology, [2]Anatomic Pathology, [3]Surgical Oncology, Tohoku University Graduate School of Medicine, Sendai; [4]Department of Pathology, Tohoku University Hospital, Sendai, Japan

(Received June 20, 2011/Revised September 15, 2011/Accepted September 27, 2011/Accepted manuscript online October 11, 2011/Article first published online November 17, 2011)

It is well-known that estrogens immensely contribute to the progression of human breast carcinoma, but their detailed molecular mechanisms remain largely unclear. In this study, we identified nucleobindin 2 (*NUCB2*) as a gene associated with recurrence based on microarray data of estrogen receptor (ER)-positive breast carcinoma cases (n = 10), and subsequent *in vitro* study showed that *NUCB2* expression was upregulated by estradiol in ER-positive MCF-7 cells. However, *NUCB2* has not yet been examined in breast carcinoma, and its significance remains unknown. Therefore, we further examined the biological functions of *NUCB2* in breast carcinoma using immunohistochemistry and *in vitro* studies. *NUCB2* immunoreactivity was detected in carcinoma cells in 77 of 161 (48%) breast cancer cases, and positively associated with lymph node metastasis and ER status of the patients. In addition, *NUCB2* status was significantly associated with an increased risk of recurrence and adverse clinical outcome of the patients using both univariate and multivariate analyses. Results of siRNA transfection experiments showed that *NUCB2* significantly increased cell proliferation, and migration and invasion properties in both MCF-7 and ER-negative SK-BR-3 cells. These results suggest that *NUCB2* is upregulated by estrogens and plays an important role, especially in the process of metastasis, in breast carcinomas. *NUCB2* status is considered a potent prognostic factor in human breast cancer. (*Cancer Sci* 2012; 103: 136–143)

Breast cancer is one of the most common malignancies in women. Estrogens play an important role in the progression of breast cancer through an interaction with ER, and ER is positive in approximately two-thirds of breast carcinoma cases. The great majority of ER-positive breast carcinomas respond to endocrine therapy such as tamoxifen and aromatase inhibitors, but it is also true that some of these carcinomas acquire clinical resistance to endocrine therapy.[1,2]

Estrogen receptor activates the transcription of various target genes in a ligand-dependent manner by binding EREs located in the promoter region. Various estrogenic functions are characterized by the expression patterns of these genes, which make it extremely important to examine the expression and roles of estrogen-responsive genes to obtain a better understanding of estrogenic actions such as progression, recurrence, and resistance to endocrine therapy.[3] Various estrogen-responsive genes have been identified in breast carcinoma,[4,5] but their detailed clinical significance and/or function remain unclear in a great majority of these genes. Therefore, in this study, we first studied the expression profiles of genes containing ERE in ER-positive breast carcinoma tissues based on microarray data, and identified *NUCB2* as a possible gene associated with recurrence in these patients.

Nucleobindin 2 has a characteristic constitution of functional domains, such as a signal peptide, a Leu/Ile rich region, two Ca^{2+} binding EF-hand domains separated by an acidic amino acid-rich region, and a leucine zipper,[6,7] and has a wide variety of basic cellular functions.[8–10] However, to the best of our knowledge, *NUCB2* has not yet been studied in breast carcinoma. Therefore, we examined *NUCB2* in breast carcinoma using immunohistochemistry and *in vitro* studies to explore its clinical and biological significance.

Materials and Methods

Patients and tissues. Two sets of tissue specimens were evaluated in this study. As a first set, 10 specimens of ER-positive breast carcinoma were obtained from women (age range, 48–74 years) who underwent surgical treatment in 2001 or 2002 in the Department of Surgery, Tohoku University Hospital (Sendai, Japan). All patients received tamoxifen therapy after surgery. The status of recurrence was evaluated whether the first locoregional recurrence or distant metastasis was detected within the follow-up time after surgery (mean, 80 months; range, 37–204 months) or not. These specimens were stored at −80°C for microarray analysis.

As a second set, 161 specimens of invasive ductal carcinoma of human breast were obtained from women who underwent surgical treatment between 1984 and 1997 in the Department of Surgery, Tohoku University Hospital. The patients did not receive chemotherapy, irradiation, or hormonal therapy before the surgery. Review of the charts revealed that 125 patients received adjuvant chemotherapy, 66 patients received tamoxifen therapy, and 12 patients received radiation therapy following surgery. The clinical outcome of the patients was evaluated by disease-free and breast cancer-specific survival. The mean age was 54 years (range, 22–81 years), and the mean follow-up time was 103 months (range, 3–157 months). Mitotic score and histological grade were evaluated according to a previous report.[11] All the specimens were fixed in 10% formalin and embedded in paraffin wax.

Research protocols for this study were approved by the Ethics Committee at Tohoku University School of Medicine (Sendai, Japan).

Laser capture microdissection/microarray analysis. Gene expression profiles of breast carcinoma cells in the first set (n = 10) were examined using microarray analysis. Gene expression profile data was assembled previously.[12,13] Briefly, approximately 5000 breast carcinoma cells were laser transferred from the frozen section, and total RNA was subsequently extracted. In this study, we focused on the expression of 519 genes identified to have a functional ERE by Bourdeau *et al.*[14]

Immunohistochemistry. Rabbit polyclonal antibody for *NUCB2* and *HER2* (A0485) were purchased from Aviva Systems Biology (San Diego, CA, USA) and Dako (Carpinteria, CA, USA), respectively. Monoclonal antibodies for ER (ER1D5), PR (MAB429), and Ki-67 (MIB1) were purchased

[5]To whom correspondence should be addressed.
E-mail: k-takagi@med.tohoku.ac.jp

doi: 10.1111/j.1349-7006.2011.02119.x

from Immunotech (Marseille, France), Chemicon (Temecula, CA, USA), and Dako, respectively.

A Histofine Kit (Nichirei, Tokyo, Japan), which incorporates the streptavidin–biotin amplification method, was used. The antigen–antibody complex was visualized with 3,3′-diaminobenzidine and counterstained with hematoxylin. Human tissue of the stomach was used as a positive control for NUCB2 antibody,[15] and normal rabbit IgG was used instead of the primary antibody, as a negative control of NUCB2 immunostaining.

NUCB2 immunoreactivity was detected in the cytoplasm of breast carcinoma cells, and the cases that had more than 10% of positive carcinoma cells were considered positive for NUCB2 status. Immunoreactivity for ER, PR, and Ki-67 was detected in the nucleus, and the immunoreactivity was evaluated in more than 1000 carcinoma cells for each case. The percentage of immunoreactivity, that is, the LI, was determined. Cases with an ER LI or PR LI of more than 10% were considered ER- or PR-positive breast carcinoma, respectively, according to a previous report.[16]

Immunoblotting. The protein of MCF-7 cells was extracted using M-PER Mammalian Protein Extraction Reagent (Pierce Biotechnology, Rockford, IL, USA) with Halt Protease Inhibitor Cocktail (Pierce Biotechnology). Twenty micrograms of the protein (whole cell extracts) was subjected to SDS-PAGE (10% acrylamide gel). Following SDS-PAGE, proteins were transferred onto Hybond-P PVDF membrane (GE Healthcare, Chalfont St Giles, UK). Primary antibody was the same anti-NUCB2 antibody used in the immunohistochemistry (Aviva Systems Biology). Antibody–protein complexes on the blots were detected using ECL Plus Western blotting detection reagents (GE Healthcare), and the protein bands were visualized with a LAS-1000 image analyzer (Fuji Photo Film, Tokyo, Japan).

Real-time PCR. Total RNA was extracted using TRIzol reagent (Invitrogen, Carlsbad, CA, USA), and cDNA was synthesized using a QuantiTect reverse transcription Kit (Qiagen, Hilden, Germany). Real-time PCR was carried out using the LightCycler System and FastStart DNA Master SYBR Green I (Roche Diagnostics, Mannheim, Germany). The primer sequences of NUCB2 and the ribosomal protein L13A (RPL13A) were: NUCB2, 5′-AAAGAAGAGCTACAACGTCA-3′ (forward) and 5′-GTGGCTCAAACTTCAATTC-3′ (reverse); and RPL13A, 5′-CCTGGAGGAGAAGAGGAAAGAGA-3′ (forward) and 5′-TTGAGGACCTCTGTGTATTTGTCAA-3′ (reverse). The NUCB2 mRNA level was calculated as the ratio of the RPL13A mRNA level.

Small interfering RNA transfection. Small interfering RNA for NUCB2 was purchased from Ambion (Austin, TX, USA). The target sequences of siRNA against *NUCB2* were as follows: si1, 5′-UAUCUUCGCACUUUCCACAGGGUGA-3′ (sense) and 5′-UCACCCUGUGGAAAGUGCGAAGAUA-3′ (anti-sense); and si2, 5′-UUGAUUAGCAUAUCUAAAUCUGUGG-3′ (sense) and 5′-CCACAGAUUUAGAUAUGCUAAUCAA-3′ (anti-sense). In addition, medium GC duplex #2 (Invitrogen) was also used as a negative control (siC). The siRNA was transfected using HiperFect transfection reagent (Qiagen).

Cell proliferation, migration, and invasion assays. MCF-7 and SK-BR-3 cells were transfected with NUCB2-specific siRNA or control siRNA in a 96-well culture plate. Three days after transfection, the cell number was evaluated using a Cell Counting Kit-8 (Dojindo, Kumamoto, Japan).

The cell migration assay was carried out using a 24-well plate and Chemotaxicell (8 μm pore size; Kurabo, Osaka, Japan) according to a previous report.[17] MCF-7 and SK-BR-3 cells were plated at the upper chamber, and the cells on the upper surface of the membrane were removed after incubation for 72 h. The migration ability was evaluated as an average number of cells in five middle power fields (×200) randomly selected on the lower surface of the membrane.

The cell invasion assay was carried out using a modified migration assay. The upper surface of the membrane of a Chemotaxicell was coated with 80 mg/cm^2 of Matrigel basement membrane matrix (BD Biosciences, Heidelberg, Germany), and the invasion ability was evaluated as the total number of cells on the lower surface of the membrane.

Results

Comparison of gene expression profiles between recurrent and non-recurrent groups of breast carcinoma patients. The microarray data used in this study are available through the National Center for Biotechnology Information Gene Expression Omnibus database (accession GSE11965, http://www.ncbi.nlm.nih.gov/geo). In this analysis, when the expression ratio of a gene in the recurrence group compared to that in the non-recurrence group was more than 2.0 or <0.5, we determined that the gene was predominantly expressed in the recurrence or non-recurrence group, respectively.

As shown in Figure 1(A), of the 519 genes examined, the number of genes predominantly expressed in the recurrence group (group A) was 17 (3%); the number of genes predominantly expressed in the non-recurrence group (group B) was 35 (7%). A great majority of the genes (467 genes; 90%) had a similar expression level in each of the two groups (ratio 0.5–2.0) (group C). The lists of genes classified in group A and group B are summarized in the right panel of Figure 1(A), and in Table S1. When we carried out gene ontology enrichment analysis between groups A and B (http://cbl-gorilla.cs.technion.ac.il/), no significant enriched gene ontology term was detected. Among the genes in Group A, *NUCB2* showed the highest ratio (4.9) and expression level, indicating its possible involvement in the recurrence in ER-positive breast carcinoma patients after surgery.

The *NUCB2* gene contains functional ERE in the promoter region[14] but the regulation of *NUCB2* expression by estradiol has not been investigated in breast carcinoma cells. As shown in Figure 1(B), NUCB2 mRNA expression was significantly increased by estradiol treatment for 3 days in MCF-7 cells. However, the NUCB2 mRNA expression level was significantly lower ($P < 0.05$, and 0.3-fold) than the basal level, when the cells were treated together with estradiol (10 nM) and a potent ER antagonist ICI 182780 (1 μM). When MCF-7 cells were treated with estradiol (10 nM) and anti-estrogen tamoxifen (10 μM), the NUCB2 mRNA level was not significantly changed compared to the basal level ($P = 0.10$, and 1.5-fold). Estradiol (10 nM) time-dependently induced NUCB2 mRNA expression in MCF-7 cells (Fig. 1C).

***NUCB2* immunolocalization in human breast carcinoma.** As shown in Figure 2(A), immunoblot analysis for *NUCB2* revealed a specific band (approximately 43 kDa) in MCF-7 cells, which confirmed the specificity of the anti-*NUCB2* antibody used in this study.[18] In the immunohistochemistry, *NUCB2* immunoreactivity was detected in the cytoplasm of breast carcinoma cells (Fig. 2B). *NUCB2* immunoreactivity was weakly and focally detected in the epithelial cells of morphologically normal glands (Fig. 2C), but it was negative in the stroma. In the positive control, *NUCB2* was mainly positive in the epithelium of the fundic glands in the stomach (Fig. 2D), as reported previously,[15] whereas no significant immunoreactivity was detected in the same areas of the negative control section (Fig. 2E).

Associations between *NUCB2* immunohistochemical status and various clinicopathological parameters in breast carcinomas are summarized in Table 1. Of 161 cases of breast carcinoma examined in this study, 77 (48%) were *NUCB2*-positive. *NUCB2* status was significantly associated with lymph node metastasis ($P = 0.004$) and ER status ($P = 0.002$) of the patients, whereas no significant association was detected in patients' age, menopausal status, clinical stage, tumor size,

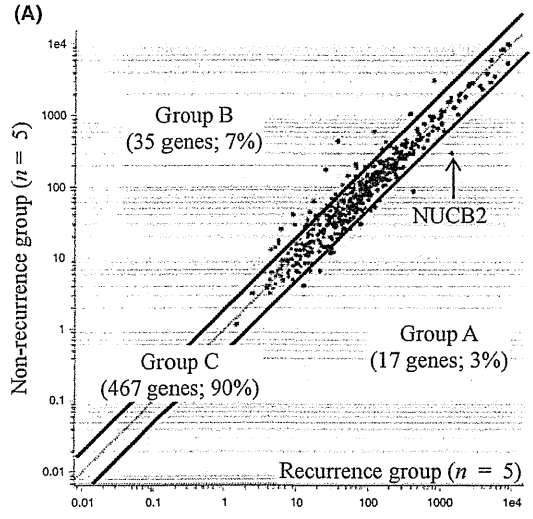

Genes classified as Group A		
Fold†	Common name	Gene symbol
4.9	**NM_005013**	**NUCB2**
4.8	AI824012	NRIP1
3.2	NM_001557	CXCR2
3.0	X02189	ADA
2.6	NM_001874	CPM
2.5	NM_001228	CASP8
2.4	AK023540	BUB1
2.3	NM_016083	CNR1
2.3	AF109161	CITED2
2.3	NM_016580	PCDH12
2.2	NM_001256	CDC27
2.2	BC005312	HLA-DRB4
2.2	AF149096	TGFA
2.1	NM_006889	CD86
2.1	X63575	ATP2B2
2.1	X81006	TRIM31
2.1	AW157548	IGFBP5

†: Expression ratio in the recurrence group to that in the non-recurrence group.

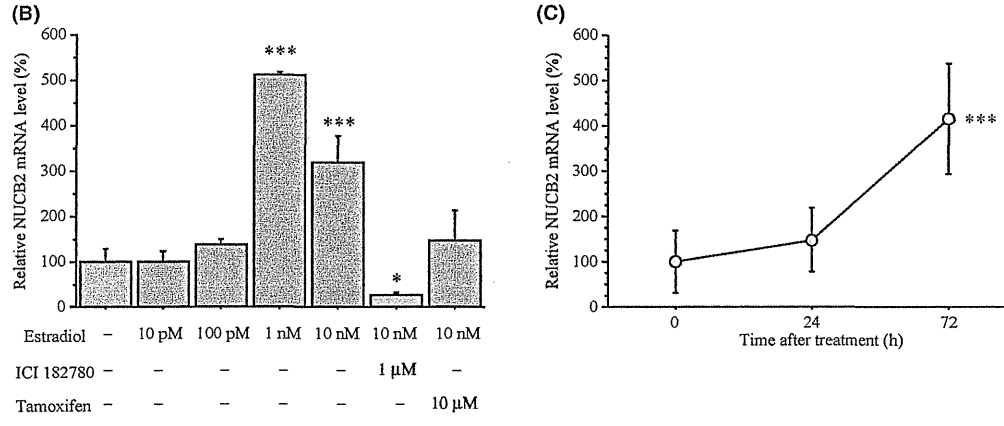

Fig. 1. Nucleobindin 2 (*NUCB2*) as an estrogen-induced gene associated with breast carcinoma. (A) Scatter plot analysis of microarray data for 519 genes containing functional estrogen-responsive element in breast carcinomas comparing the recurrence and non-recurrence group (n = 5 in each group). Genes with an expression ratio, recurrence group to non-recurrence group, of more than 2.0 or <0.5 are located outside the diagonal line, and classified as group A or group B, respectively. Genes with a ratio between 2.0 and 0.5 were classified as group C. *NUCB2* showed the highest ratio in these genes (arrow). The right panel summarizes the gene list of group A. (B,C) Effects of estradiol on NUCB2 mRNA expression. MCF-7 cells were treated with indicated concentrations of estradiol with or without (–) ICI 182780 or tamoxifen for 3 days (B) or treated with estradiol (10 nM) for the indicated period (C). The relative NUCB2 mRNA level summarized as a ratio (%) compared with the basal level (non-treatment). Data are presented as the mean ± SD (n = 3). *P < 0.05 and ***P < 0.001 versus non-treatment (left bar) (B) or 0 h (left plot) (C).

histological grade, mitotic score, PR status, *HER2* status, or Ki-67 LI. The positive association between *NUCB2* status and lymph node metastasis was significant regardless of the ER status of these cases (P = 0.02) (Table S2). *NUCB2* status was positively associated with Ki-67 LI in the ER-positive group (P = 0.02), and was positively correlated with tumor size in ER-negative cases (P = 0.03).

When immunohistochemistry was carried out in ductal carcinoma *in situ*, *NUCB2* immunoreactivity was detected in the carcinoma cells (Fig. 2F) in 7 (32%) of 22 cases. The *NUCB2* positivity was 1.5-fold higher in invasive carcinoma (48%) than non-invasive carcinoma (32%), although it did not reach a level of significance (P = 0.15).

Association between *NUCB2* status and clinical outcome. In order to thoroughly examine the association between *NUCB2* status and patient prognosis, we excluded stage IV cases and used stage I–III breast carcinoma patients (n = 141) in the following analyses. As shown in Figure 3(A), *NUCB2* status was significantly associated with an increased incidence of recurrence (P = 0.003), and the multivariate analysis revealed that lymph node metastasis (P = 0.01), ER status (P = 0.002), and *NUCB2* status (P = 0.001) were independent prognostic factors for disease-free survival with relative risks over 1.0 (Table 2).

A breast cancer-specific survival curve of the patients is summarized in Figure 3(B); a significant correlation (P = 0.0002) was detected between *NUCB2* status and adverse clinical outcome in the 141 breast carcinoma patients examined. In the univariate analysis (Table 2), lymph node metastasis (P = 0.0004), *NUCB2* status (P = 0.002), ER status (P = 0.003), histological grade (P = 0. 01), *HER2* status (P = 0.01), and tumor size (P = 0.02) were all indicated as significant prognostic variables for breast cancer-specific survival. A following multivariate analysis showed that only *NUCB2* status (P = 0.0004) and ER status (P = 0.01) were independent prognostic factors with a relative risk over 1.0, whereas lymph node metastasis

doi: 10.1111/j.1349-7006.2011.02119.x

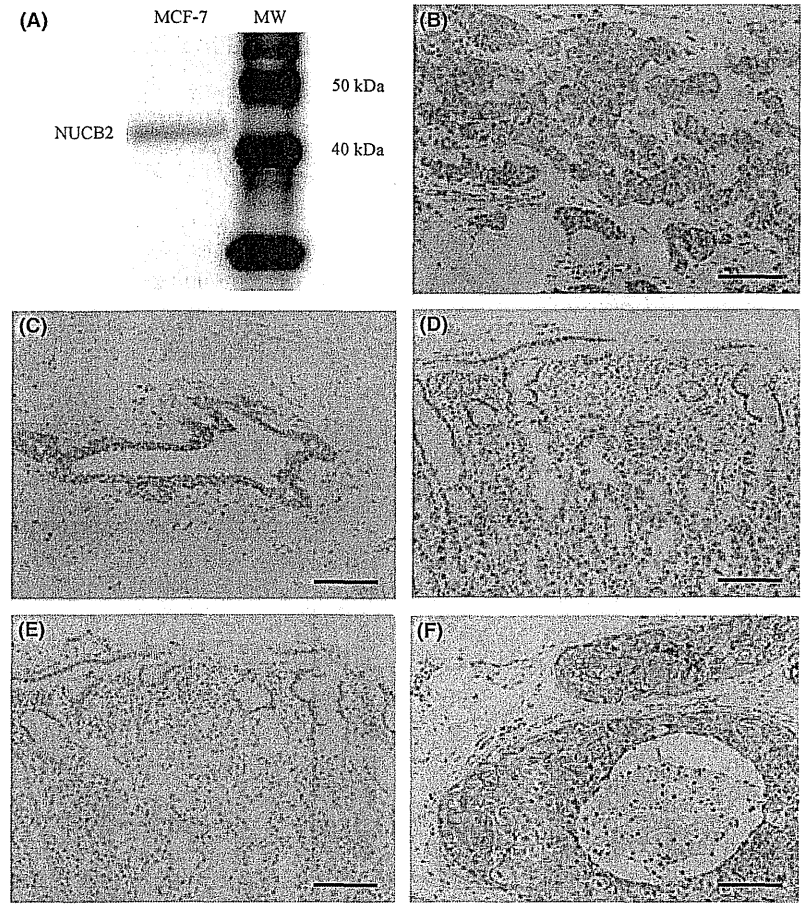

Fig. 2. Immunohistochemistry for nucleobindin 2 (*NUCB2*) in breast carcinoma. (A) Immunoblotting for *NUCB2* in MCF-7 cells. MW, molecular weight. (B) *NUCB2* immunoreactivity was detected in the carcinoma cells of invasive ductal carcinoma. (C) *NUCB2* immunoreactivity was weakly and focally detected in morphologically normal mammary glands. (D) Positive control section of *NUCB2* immunohistochemistry (gastric mucosa). (E) Negative control section of *NUCB2* immunohistochemistry (same area as Fig. 2D). (F) *NUCB2* immunoreactivity was detected in the carcinoma cells of ductal carcinoma *in situ*. Bar = 100 μm.

($P = 0.22$), histological grade ($P = 0.28$), *HER2* status ($P = 0.60$), and tumor size ($P = 0.07$) were not significant.

A similar association between *NUCB2* and worse prognosis was detected regardless of the Ki-67 status ($P = 0.03$ in cases with Ki-67 LI ≥ 10% and $P = 0.04$ in cases with Ki-67 < 10% for disease-free survival [Fig. 3C]; $P = 0.004$ in cases with Ki-67 LI ≥ 10% and *P*-value not available cases with Ki-67 < 10% because no patient died in the *NUCB2*-negative group for breast cancer-specific survival). When the 66 *NUCB2*-positive cases were further categorized into two groups according to immunointensity (++, strongly positive [$n = 16$]; +, modestly positive [$n = 50$]), no significant difference was detected between these two groups ($P = 0.60$ for disease-free survival [Fig. 3D], and $P = 0.49$ for breast cancer-specific survival).

Forty patients with stage I–III disease received tamoxifen therapy following surgery as an adjuvant treatment, and these cases were all positive for ER. *NUCB2* status was also markedly associated with an increased risk of recurrence (Fig. 3E) and worse prognosis (data not shown) in the patients who received tamoxifen therapy, although *P*-values were not available because no patient had recurrent disease or died in the group of *NUCB2*-negative cases. Significant association between *NUCB2* status and patients' clinical outcome was also detected in the 113 patients who received adjuvant chemotherapy ($P = 0.03$ for disease-free and $P = 0.002$ for breast cancer-specific survival), 38 ER-negative cases ($P = 0.0001$ for disease-free and $P < 0.0001$ for breast cancer-specific survival), or 24 cases with ER LI < 1% ($P = 0.001$ for disease-free [Fig. 3F] and $P = 0.0004$ for breast cancer-specific survival).

Effects of *NUCB2* expression on cell proliferation and invasion in breast carcinoma cells. The results of our study suggest that *NUCB2* is associated with worse prognosis of breast carcinoma patients regardless of their ER status, although *NUCB2* expression is upregulated by estrogen. In order to further examine the biological functions of *NUCB2* in human breast carcinoma, we transfected specific siRNA for *NUCB2* both in ER-positive MCF-7 and ER-negative SK-BR-3 breast carcinoma cells. The NUCB2 mRNA expression level was markedly decreased in these cells transfected with specific *NUCB2* siRNA (si1 or si2) at 3 days after transfection compared to cells transfected with control siRNA (siC). The ratio of NUCB2 mRNA level compared to that in the control siRNA was: MCF-7, 5% (si1) and 8% (si2); and SK-BR-3, 11% (si1) and 12% (si2).

As shown in Figure 4(A), the number of cells was significantly lower in MCF-7 cells transfected with *NUCB2* siRNA ($P < 0.001$ and 0.52-fold in si1, and $P < 0.001$ and 0.64-fold in si2) than in control cells transfected with siC 3 days after the transfection. A similar association was also detected in SK-BR-3 cells under the same conditions ($P < 0.001$ and 0.75-fold in si1, and $P < 0.001$ and 0.81-fold in si2). Figure 4(B) shows the

Table 1. Association between nucleobindin 2 (*NUCB2*) immunohistochemical status and clinicopathological parameters in 161 breast carcinomas

	NUCB2 status		*P*-value
	Positive (n = 77)	Negative (n = 84)	
Age† (years)	53.9 ± 1.4	54.4 ± 1.2	0.770
Menopausal status (%)			
Premenopausal	31 (19)	35 (22)	0.860
Postmenopausal	46 (29)	49 (30)	
Stage (%)			
I	18 (11)	24 (15)	0.730
II	38 (24)	43 (27)	
III	10 (6)	8 (5)	
IV	11 (7)	9 (6)	
Tumor size† (cm)	3.4 ± 0.4	3.4 ± 0.4	0.990
Lymph node metastasis (%)			
Positive	41 (25)	26 (16)	**0.004**
Negative	36 (22)	58 (36)	
Histological grade (%)			
1 (well)	20 (12)	24 (15)	0.930
2 (moderate)	30 (19)	31 (19)	
3 (poor)	27 (17)	29 (18)	
Mitotic score (%)			
1 (low)	33 (20)	43 (27)	0.570
2 (moderate)	22 (14)	21 (13)	
3 (high)	22 (14)	20 (12)	
ER status (%)			
Positive	65 (40)	53 (33)	**0.002**
Negative	12 (7)	31 (19)	
PR status (%)			
Positive	55 (34)	51 (32)	0.150
Negative	22 (14)	33 (20)	
HER2 status (%)			
Positive	22 (14)	24 (15)	0.990
Negative	55 (34)	60 (37)	
Ki-67 LI† (%)	23.6 ± 1.8	21.1 ± 2.1	0.380

†Data are presented as the mean ± SEM. All other values represent the number of cases and percentage. ER, estrogen receptor; LI, labeling index; PR, progesterone receptor. *P*-values <0.05 were considered significant, indicated in bold.

results of the migration assay. The number of migrated cells was significantly lower in both MCF-7 cells ($P < 0.001$ and 0.11-fold in si1, and $P < 0.001$ and 0.43-fold in si2) and SK-BR-3 cells ($P < 0.001$ and 0.36-fold in si1, and $P < 0.001$ and 0.31-fold in si2) transfected with *NUCB2* siRNA than in those transfected with control siRNA at 1 day (MCF-7) or 2 days (SK-BR-3) after the transfection. Moreover, the number of invaded cells was also significantly lower in the cells transfected with *NUCB2* siRNA (MCF-7, $P < 0.05$ and 0.21-fold in si1 and $P < 0.05$ and 0.29-fold in si2; SK-BR-3, $P < 0.01$ and 0.66-fold in si1 and $P < 0.001$ and 0.47-fold in si2) (Fig. 4C,D).

Discussion

Gene expression profiling is an important method to predict the likelihood of recurrence of disease in breast cancer patients,[19] in addition to conventional clinical and histopathological examination. A multigene classifier associated with recurrence has been proposed for breast carcinoma patients by several research groups,[19–21] and molecular-based diagnostic systems have been developed, such as MammaPrint[22] and Oncotype DX,[23] as well as the genomic grade index.[24] However, the selected genes vary markedly between these diagnostic systems, which may be partly due to the fact that they use different platforms for the analysis of gene expression. In addition, the biological functions have remained largely unknown in a great majority of these genes. In our present study, the results of microarray analysis revealed 17 genes that are potentially associated with recurrence in ER-positive breast carcinoma patients (group A in Fig. 1A). Among these, *IGFBP5* (insulin-like growth factor-binding protein 5) was reported to play an important role in breast carcinoma metastasis,[25,26] and is included in MammaPrint. In addition, *TGFA* (transforming growth factor α), a member of the epidermal growth factor family, is well-known to be involved in cellular proliferation and carcinogenesis.[27] The kinetochore-bound protein kinase *BUB1* (budding uninhibited by benzimidazoles 1) is a possible link to tumorigenesis.[28] *NUCB2* showed the highest expression ratio in this study, but this gene has not been listed in any multigene classifiers predicting breast carcinoma recurrence, nor has it been examined in breast carcinoma, to the best of our knowledge.

In this study, we first showed that *NUCB2* immunoreactivity was detected in 48% of breast carcinoma cases, although levels were almost negligible in morphologically normal mammary glands. *NUCB2* is known to mainly express in key hypothalamic nuclei with proven roles in energy homeostasis.[9] Moreover, recent investigations have indicated that *NUCB2* is also expressed in various human peripheral tissues, including the stomach, pancreas, reproductive organs, and adipose tissues, with relevant metabolic functions, suggesting that *NUCB2* signaling might participate in adaptative responses and in the control of body functions gated by the state of energy reserves.[29] However, *NUCB2* expression in carcinoma has only been examined in the stomach; Kalnina *et al.*[15] reported that *NUCB2* immunoreactivity was not detected in carcinoma cells in 15 gastric carcinoma cases examined. The relatively wide distribution of *NUCB2* immunoreactivity in our present study suggests that *NUCB2* plays an important role in human breast carcinoma.

Bourdeau *et al.*[14] evaluated genome-wide identification of EREs in humans, and identified a functional ERE element at 8257 bp from the most upstream mRNA 5′-end of the *NUCB2* gene. In our present study, *NUCB2* immunohistochemical status was positively associated with ER status in breast carcinoma tissue, and NUCB2 mRNA was significantly upregulated by estradiol in MCF-7 cells through ER. Therefore, *NUCB2* is considered one of the estrogen-induced genes in breast carcinoma cells. Results of our present study also indicated the presence of *NUCB2* in 12 of 43 (28%) ER-negative breast carcinoma cases; it might be the case that *NUCB2* was induced by a low or undetectable level of ER in these cases. However, it is also true that estrogen-mediated induction of NUCB2 mRNA was relatively slow in MCF-7 cells in our time-course study (Fig. 1C), suggesting that *NUCB2* expression is, at least in a part, induced by secondary responses, although the half-life of mRNA is an important factor in determining how long it takes to detect a change in the mRNA level of a specific gene.[4] In addition, *NUCB2* is expressed in various human tissues not necessarily considered targets for estrogens, as described above.[29] Therefore, other factors than estrogens might be involved in the expression of *NUCB2* in breast carcinoma cells. No information is currently available regarding the regulation mechanisms of *NUCB2* expression to the best of our knowledge, and further research is required.

Previous studies have shown that ICI 182780 possesses a greater ability to suppress estrogen-sensitive gene expression and greater antitumor activity than tamoxifen in breast carcinoma.[30] This is partly due to the fact that ICI 182780 does not have agonistic ER activity and reduces steady-state levels of ER by increasing the turnover of the protein, whereas tamoxifen does possess partial agonistic ER activity.[31] In our study, ICI 182780 was superior to tamoxifen in suppressing estradiol-mediated induction of NUCB2 mRNA in MCF-7 cells (Fig. 1B), which is consistent with previous studies.

doi: 10.1111/j.1349-7006.2011.02119.x